AD-A139 196 APPLICATION OF RAPIDLY SOLIDIFIED SUPERALLOYS(U) PRATT AND WHITNEY AIRCRAFT GROUP WEST PALM BEACH FL A R COX 14 MAY 76 PWA-FR-7627 F33615-76-C-5136 1/1

UNCLASSIFIED F/G 11/6 NL

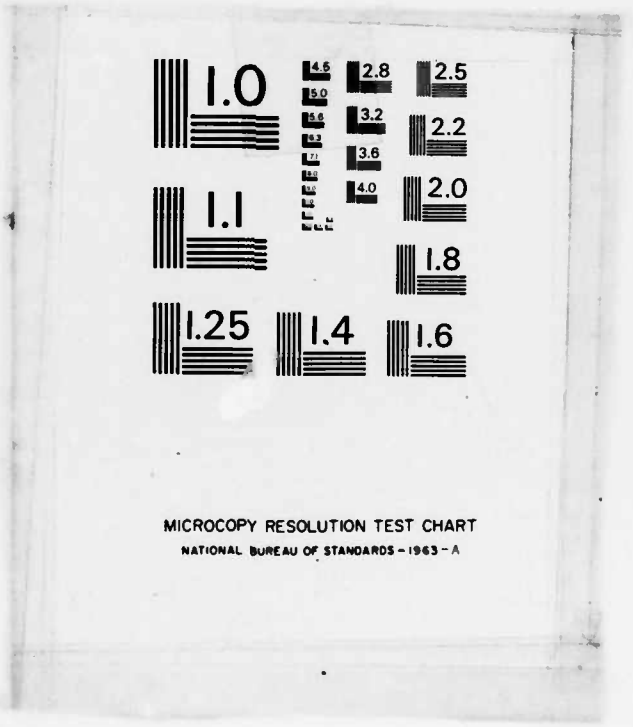
1.0
4.6
5.0
5.6
2.8
2.5
3.2
2.2
3.6
4.0
2.0
1.1
1.8
1.25
1.4
1.6
MICROCOPY RESOLUTION TEST CHART
NATIONAL BUREAU OF STANDARDS - 1963 - A

Pratt & Whitney Aircraft

UNCLASSIFIED

SECURITY CLASSIFICATION OF THIS PAGE *(When Data Entered)*

| REPORT DOCUMENTATION PAGE | | READ INSTRUCTIONS BEFORE COMPLETING FORM |
|---|---|---|
| 1. REPORT NUMBER | 2. GOVT ACCESSION NO. AD-A139196 | 3. RECIPIENT'S CATALOG NUMBER |
| 4. TITLE *(and Subtitle)*<br>APPLICATION OF RAPIDLY SOLIDIFIED SUPERALLOYS | | 5. TYPE OF REPORT & PERIOD COVERED<br>Quarterly<br>1 February - 30 April 1976 |
| | | 6. PERFORMING ORG. REPORT NUMBER<br>FR-7627 |
| 7. AUTHOR(s)<br>A.R. Cox | | 8. CONTRACT OR GRANT NUMBER(s)<br>F33615-76-C-5136 |
| 9. PERFORMING ORGANIZATION NAME AND ADDRESS<br>United Technologies Corporation<br>Pratt & Whitney Aircraft Group<br>Box 2691, West Palm Beach, Florida 33402 | | 10. PROGRAM ELEMENT, PROJECT, TASK AREA & WORK UNIT NUMBERS |
| 11. CONTROLLING OFFICE NAME AND ADDRESS<br>Defense Advanced Research Projects Agency<br>1400 Wilson Boulevard<br>Arlington, Virginia 22209 | | 12. REPORT DATE<br>14 May 1976<br>13. NUMBER OF PAGES<br>44 |
| 14. MONITORING AGENCY NAME & ADDRESS*(If different from Controlling Office)*<br>Air Force Materials Laboratories<br>Wright-Patterson AFB, Ohio 45433 | | 15. SECURITY CLASS. *(of this report)*<br>Unclassified<br>15a. DECLASSIFICATION/DOWNGRADING SCHEDULE |

16. DISTRIBUTION STATEMENT *(of this Report)*

Approved for Public Release, Distribution Unlimited

17. DISTRIBUTION STATEMENT *(of the abstract entered in Block 20, if different from Report)*

18. SUPPLEMENTARY NOTES

19. KEY WORDS *(Continue on reverse side if necessary and identify by block number)*

Superalloys, Powder Metallurgy, Rapid Solidification, Turbine Airfoils, Centrifugal Atomization, Convective Cooling

20. ABSTRACT *(Continue on reverse side if necessary and identify by block number)*

This program is being conducted for the purpose of applying the principle of fast solidification to superalloy powders and subsequent development of stronger compositions for jet engine turbine airfoils. Centrifugal atomization and forced convective cooling of the material are being used for producing the fast cooled material. During this report period, conditions for stable operation of the device used for fast cooling were investigated, and material thus produced was evaluated

DD FORM 1 JAN 73 1473 EDITION OF 1 NOV 65 IS OBSOLETE

UNCLASSIFIED

SECURITY CLASSIFICATION OF THIS PAGE *(When Data Entered)*

with respect to the effect of fast cooling on microstructure. It was found that molten metal stream stability is a fundamental requirement for useful operation. High tangential velocities of the atomized metal are required for high yields of fast cooled powder. Cooling rates in excess of $10^5$°C/sec are attainable for IN100 alloy powder. IN100 alloy cooled at these rates exhibited a total suppression of the $\lambda'$ phase and significant suppression of the primary carbide phase. Product quality commensurate with present quality standards for superalloy powder appears attainable.

## SUMMARY

This program is being conducted for the purpose of applying the principle of fast solidification to superalloy powders and subsequent development of stronger compositions for jet engine turbine airfoils. Centrifugal atomization and forced convective cooling of the material are being used for producing the fast cooled material. During this report period, conditions for stable operation of the device used for fast cooling were investigated, and material thus produced was evaluated with respect to the effect of fast cooling on microstructure. It was found that molten metal stream stability is a fundamental requirement for useful operation. High tangential velocities of the atomized metal are required for high yields of fast cooled powder. Cooling rates in excess of $10^5$°C/sec are attainable for IN100 alloy powder. IN100 alloy cooled at these rates exhibited a total suppression of the $\gamma'$ phase and significant suppression of the primary carbide phase. Product quality commensurate with present quality standards for superalloy powder appears attainable.



| Accession For | |
|---|---|
| NTIS GRA&I | ☑ |
| DTIC TAB | ☐ |
| Unannounced | ☐ |
| Justification | |
| By | |
| Distribution/ | |
| Availability Codes | |
| Dist | Avail and/or Special |
| A-1 | |

CONTENTS

# ILLUSTRATIONS

ILLUSTRATIONS (Continued)

# SECTION I
# INTRODUCTION

The strongest superalloy turbine airfoil used in today's most advanced jet engine is cast from a composition developed more than 15 years ago. This composition is the alloy Mar M 200, and the application is in the Pratt & Whitney Aircraft F100 engine, which is used in the F-15 and F-16 aircraft. Better component design and better materials processing have enabled significant gains in jet engine performance since the alloy was introduced; however, it is apparent that further improvement in turbomachinery will require better superalloys than now available.

The major contributing factor to this 15-year period of no alloy improvement has not been the lack of development interest; every major aerospace organization has performed intensive efforts to circumvent this stoppage. Rather, it appears that the boundary conditions imposed by the exclusive use of vacuum-induction melting and vacuum arc (or electroslag) remelting for alloy improvement have been reached and cannot be expanded without a change to this very basic mode of processing. These boundary conditions appear in the form of chemical segregation of ingot or casting, which subsequent solid-state operations do not eliminate. Owing to this segregation are such alloy conditions as instability in the form of TCP phases, reactions to massive carbide, eutectic formations, and low incipient melting temperature. Each is known to cause degradation in alloy strength.

Superalloy powder metallurgy studies conducted by P&WA/Florida show that the use of powder, particularly powder solidified at very high rates of cooling, can circumvent chemical segregation and eliminate the present boundary conditions imposed by conventional melting practices. Suppression of sigma phase has been observed in high Ti $\gamma'$ alloy powders cooled near $10^{2}$°C/sec, suppression of $\eta$ observed in high Ti/Al ratio alloys at rates near $10^{3}$°C/sec, and suppression of both carbide and $\gamma'$ observed in high C, high Al alloys at rates near $10^{5}$°C/sec. All of these reactions are noted in ingot, which typically solidifies and cools at rates near $10^{-2}$°C/sec. Also, for each of the powder cases cited above, incipient melt temperatures are higher than ingot products of the same compositions, and massive formations of eutectic $\gamma'$, common to ingot, do not occur. These observations clearly show that powder metallurgy methods can, in fact,

circumvent the boundary limits of ingot casting and can be used as a basic mode of processing to develop stronger superalloys than the Mar M 200 composition.

The use of superalloy powder has proved to be a viable production method that can meet the most demanding quality standards, as attested to by the fact that the F100 bill-of-material high compressor and turbine disks are produced from superalloy powder. Further, superalloy powder metal components that have been forged by the GATORIZING™ process can be subsequently heat treated in a manner to effect abnormal grain growth, a condition that significantly improves material strength at temperatures above 1/2 $T_m$. Mechanical tests with Mar M 200 alloy, in fact, have shown that GATORIZED Mar M 200 powder (after heat treating) is as strong or stronger than the same composition cast in a directional mode.

P&WA/Florida has constructed a powder device that can produce metal powders solidified and cooled at rates near $10^6$°C/sec. The underlying principal is forced convective cooling, whereby powder particles of controlled size are accelerated into a high thermal conductivity gaseous medium maintained at high $\Delta T$ between itself and the metal particle.

The purpose of this ARPA-sponsored program is to refine the process mechanics used with the powder producing device for fast quenching bulk lots of powder and, subsequently, apply the technology of rapid solidification to the development of an alloy composition that is stronger than the existing Mar M 200 alloy and that can be implemented for the production of better turbine airfoils.

The program is a 40-month effort and is organized as a progression of events starting with a parametric study of the requirements necessary to achieve high yields of fast quenched powder and terminating in the fabrication and testing of turbine airfoils. This report is the first technical report and covers the first 3 months of the program. It deals exclusively with the study of producing fast quenched superalloy powder and includes observations on resulting material characteristics.

## SECTION II
## PROCESS MECHANICS

In previous work conducted at P&WA/Florida, a series of analytical and experimental studies were carried out in an effort to define a means for production of fast quenched powders that could be implemented with a minimum amount of technological development. Several prerequisites were apparent. First, any useful approach would have to be capable of providing materials in significant quantities; second, the material produced should adapt itself to simple screening techniques for uniformity of cooling rate; third, the material should be easily handled; and, fourth, for subsequent operation, the material should have inherently high pour density and good flow characteristics.

Initial work paralleled that of many investigators in attempting to attain high quench rates by conductive heat removal from the solidifying bodies. Although the results showed the attainment of desired cooling speeds, the material thus produced exhibited variations in size and thickness (leading to variations in cooling rate) and, at no time, could a steady-state operation be achieved. Particle adherence to, and erosion of, the conducting heat sink were the principle problems encountered. None of the above criteria were satisfied in any of the attempts made.

Concurrent analytical work, however, showed that forced convection cooling, adequately controlled, could be used to produce powders quenched at fast rates. In fact, the rates possible were analytically determined to be within an order of magnitude of the theoretical limit for "splat" (1-dimensional heat transfer) and within about 2-3 orders of magnitude of the theoretical limit for any method (3-dimensional heat transfer). This relationship is shown in figure 1.

The analytical model used to derive the cooling capacity of gas quenching media was based on the use of a particle generator that was itself capable of producing spherical particles and accelerating them into a quenching environment. The incremental heat lost by such particles at temperature $T_p$ can be expressed as

$$\frac{\Delta H}{\Delta t} = hA\left(T_p - T_g\right) + A\epsilon\sigma\left(T_p^4 - T_w^4\right)$$

where

A = surface area of particle

h = interfacial heat transfer coefficient

$\epsilon$ = emissivity of the material

$\sigma$ = Stefan-Boltzmann constant

$T_g$ = temperature of the local environment

$T_w$ = background temperature

For spherical particles of diameter d, h can be expressed as $h = \frac{KNu}{d}$, while $A = \pi d^2$, where K = thermal conductivity of the environment and Nu = dimensionless Nusselt number.

The Nusselt number has been empirically determined by a number of investigators in the field of heat transfer and is of the form $Nu = a + bPr^m Re^n$, where Pr is the Prandtl number and Re the Reynolds number; the former has been determined for a variety of gases and may be obtained from tables of gas properties, while the latter has the form $Re = \frac{\rho V d}{\mu}$ where V = relative velocity, $\rho$ = density of the gas, and $\mu$ = dynamic viscosity.

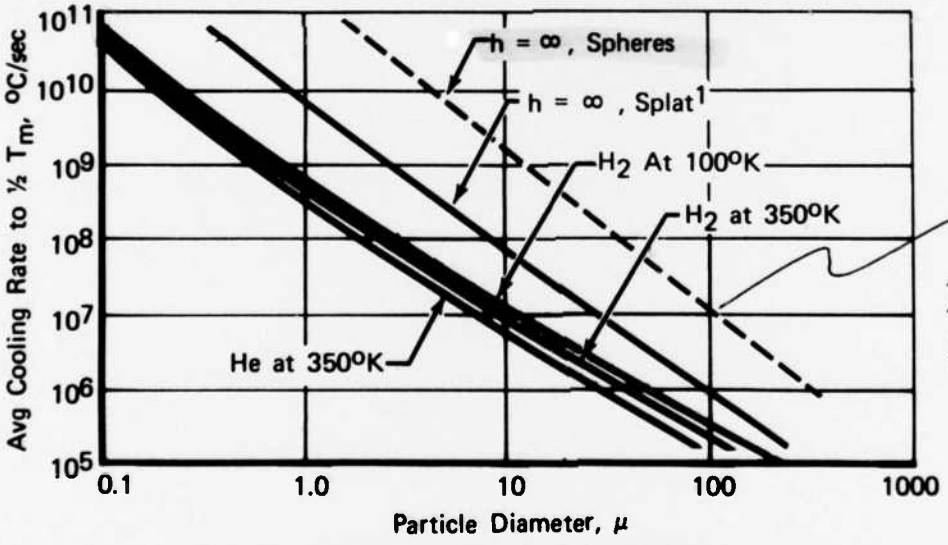


[1]Ruhl, RC, "Cooling Rates in Splat Cooling", Materials Science and Engineering, Vol 1, 1967, Pg 313

Figure 1. Cooling Rates Possible by Forced Convection Compared to Theoretical Limits

FD 92937

Investigators in heat transfer have reported good correlations of the Nusselt number for spherical particles with $a = 2$ and with $1/2 \leq b \leq 2/3$, $m = 1/3$, and $n = 1/2$, for $2 \leq Re \leq 800$. Although the majority of cases of interest have $2 \leq Re \leq 400$, $b = 1/3$ was selected to produce conservative results.

Substitution of the pertinent expressions yields:

$$\frac{\Delta H}{\Delta t} = \pi dK \left[ 2 + 1/3 \, Pr^{1/3} \left( \frac{\rho V d}{\mu} \right)^{1/2} \right] \left( T_p - T_g \right) + \pi d^2 \epsilon \sigma \left( T_p^4 - T_w^4 \right)$$

where the first expression on the right of the equality relates heat transferred from the particles by forced convection, while the second relates heat transferred by radiation during the time increment $\Delta t$. In the latter term, for a given material, only the particle diameter and initial temperature can be conveniently varied and, for materials and particle sizes of interest, the term is relatively small when compared to the forced-convection term. Examination of this term implies that the important parameters are the properties of the gas, the particle size, the relative (particle-gas) velocity, and the temperature (particle-gas) difference; the actual temperature change of a particle depends upon its size and the heat capacity of the material at $T_p$. One can then calculate the heat content at the beginning of the time increment, the approximate heat lost during the increment and, thus, the new temperature of the particle at the end of the time increment.

Calculations for this purpose were carried out by computer since the equation must be solved simultaneously with the equations of motion. Also, the relative velocity of the particles and gas is not constant but is a function of gas and particle velocities, drag, acceleration of gravity, and the properties of the gas. Too, the heat capacity of the material is a function of temperature, and the temperature is a function of time.

For several reasons, it is not appropriate to say that the predictions rendered by this technique are exact. First, the heat capacity and emissivity, as functions of temperature, are not known over a wide enough range for most materials and necessitate extrapolation. Second, the degree of undercooling that might occur was not known and could well vary as a function of cooling rate and particle size. Too, there have been some reports in the literature that indicate that under sufficiently high cooling rates, the heat of fusion may not be released. Also, in the actual situation, a range of particle sizes is likely

to be encountered, and, as these particles will decelerate and cool at different rates, they may interfere with one another.

This model does allow, however, evaluation of the relative merits of gas type, pressure, temperature, and velocity; and particle size, initial temperature, and velocity. Other effects on cooling rate, such as suppression of the release of the heat of fusion and the degree of undercooling, can also be studied.

The accuracy of the model is good, subject to the constraints mentioned. The majority of programming was conducted with the straightforward Euler technique and single precision on an IBM 360. Comparison with a run incorporating a quartic Runge-Kutta technique and double precision implied that errors due to "roundoff" and the Euler technique amounted to less than 15% for the finest particles and to less than 5% for the coarser particles. Though conduction within the particle has been neglected, the effect on mean cooling rate predictions for alloys of the superalloy type was trivial. A finite difference technique was used to consider the case where the interfacial heat transfer coefficient was infinite and the cooling of the particle was conduction limited. The rates obtaincd for this case approached three orders of magnitude higher than the practical rates predicted for helium. Thus, since the heat can be conducted to the surface much faster than it can be removed through the interface, the particles are essentially uniform in temperature, and conduction within the particle can be neglected.

While the program can calculate trajectories and cooling rates for any desired particle size, it relies on macroscopic interaction of the gas, and the predictions are not expected to be valid when particle size approaches the mean free path length of the quench gas molecules; for helium near STP, this is about 0.19 $\mu$, while for hydrogen near STP this amounts to 0.12 $\mu$. This was not considered a problem, however, since the sizes of interest occurred in the 10 $\mu$ - 200 $\mu$ range. It should be noted further that the approach was restricted to the action of the gas on the particles, and was thus applicable to powder making processes only where the gas and particle velocities were high enough and the powder production rate low enough that the action of the particles on the gas and on each other could be neglected.

The initial studies considered argon, helium, and hydrogen at mean pressures of 1, 5, and 10 atmospheres. Gas velocities selected ranged from 0 to

0.7 Mach, with an inlet gas temperature of 350K. IN-100 alloy, in particle sizes from 10 $\mu$ to 200 $\mu$ diameter, was selected for study, with particle velocities of 50 m/sec and 100 m/sec. An undercooling of $\sim$ 0.075 the normal liquidus was presumed. Mean cooling rates were calculated from the presumed liquidus to 0.5 that temperature.

Initial studies indicated that hydrogen and helium were superior to argon by more than one order of magnitude in mean cooling rate, and argon was therefore dropped from contention as a desirable quench environment.

These studies also emphasized that particle size was the most significant variable affecting cooling rate, with gas type second and mean gas pressure, inlet temperature, and relative particle-gas velocity having minor contributions. It should be noted that by minor, it is meant that modest variations of these variables had signficantly less effect on mean cooling rate than did comparable changes in particle size or type of gas. For example, the study indicated that a 50 $\mu$ particle cooled by hydrogen at 600 m/sec, 5 atmospheres mean pressure, and 350K inlet temperature would have a mean cooling rate of about $6.5 \times 10^5$°C/sec. Decreasing the inlet temperature to 100K (which is a 70% reduction in the inlet temperature) results in a cooling rate of $8.2 \times 10^5$°C/sec, while a 20% increase in particle size results in a cooling rate of $4.6 \times 10^5$°C/sec. The former represents a change in cooling rate of approximately 26%, while the latter represents a change about 30%.

On this basis (that gas quenching can achieve cooling rates commensurate with those generally associated with "splat"), the study was taken further to define a practical means for implementation and proof testing.

A central rotary atomizer was selected as the best means for producing the particles because, under this condition, particle generation and size control could be isolated to a single entity. In nonrelated industry usage, rotary (centrifugal) atomization has proved to be an effective means for steady-state production of particles and can be used to produce a narrow particle size distribution, a desirable feature from a high yield point of view. Generally, atomizers of this type have been used to produce coarse powder materials, but only because of physical limitations with respect to speed and mass flowrate.

Emperical relations have been derived for rotary atomizers that take the form of

$$d = K\left(\frac{\dot{M}^{0.2}}{r^{0.3}\,\omega^{0.6}}\right)\left(\frac{\sigma^{0.1}\,\mu^{0.2}}{\rho^{0.5}}\right)$$

physical properties of molten droplet

where d = mean particle diameter (surface/volume)

K = constant

$\dot{M}$ = mass flowrate

r = atomizer radius

$\omega$ = rotational speed

$\sigma$ = surface tension

$\mu$ = viscosity

$\rho$ = density

From experimental work conducted for wetted (coupled) surfaces, K = 1/3. For IN100-type material, the relationship of anticipated mean particle sizes to rotational speed is shown graphically in figure 2. Three flowrates are depicted for two atomizing diameters.

The particle size range of interest falls into a convenient speed range of 15,000-35,000 rpm. Calculated horsepower to accelerate the liquid metal was small, on the order of 10 hp and less. A requirement of this magnitude was considered well within the state-of-the-art for today's turbomachinery.

A prototype device incorporating these principles of rotary atomization and forced convective cooling was constructed to test the feasibility of fast quenching in a gaseous medium. The rig, designated AGT400,000, is illustrated in figure 3 and is capable of handling metal charges up to 23 kilograms (based on nickel). Principal design parameters were based on metal atomization rates of about 151 grams per sec. The gas nozzle assemblies were constructed and located in a manner to maintain a high $\Delta T$ and velocity profile for the solidifying particles relative to the gas itself.

Initial trial runs with IN100 alloy confirmed that predicted cooling rates could be achieved.

Production: $\simeq 20\#/\text{min} \simeq 1200\#/\text{hr} \simeq 28800\#/\text{day} = 14\text{T/day}$

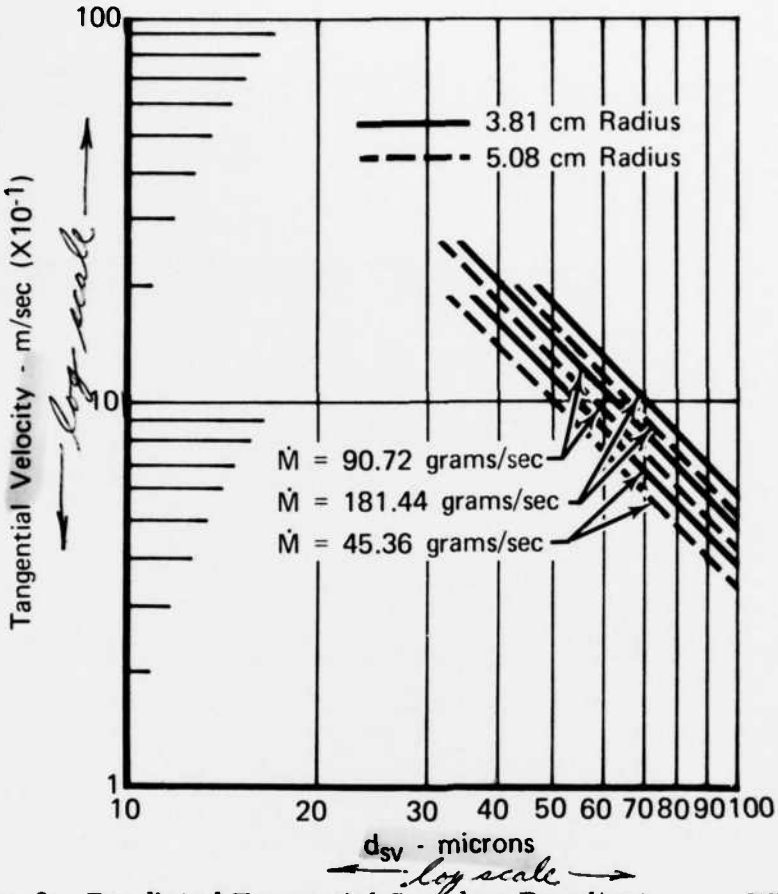


Figure 2. Predicted Tangential Speed vs Resultant Particle Size for IN100-Type Material FD 98316

The effort expended during this report period was directed toward defining control limits, environmental effects, and regions of criticality for stable operation. Seventeen runs were made during this period for this purpose. All runs were made with IN100 alloy, an alloy of nominal composition 9.5% Cr, 15.0% Co, 4.5% Ti, 5.5% Al, 3.0% Mo, 1.0% V, 0.17% C, 0.06% Zr, 0.02% B, and the balance Ni. In breaking down the sequence of operations, categorization can be made as follows:

- Melting
- Pouring
- Atomization
- Quenching
- Collection

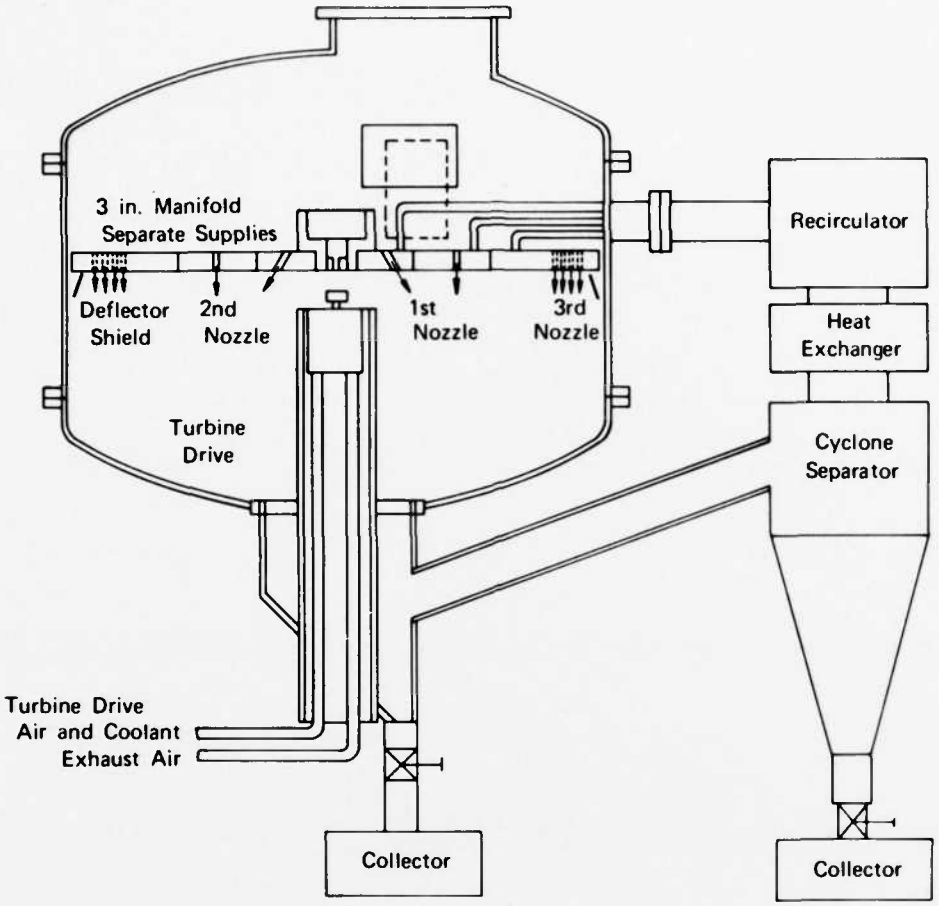


Figure 3. Experimental Powder Rig FD 92738

The following paragraphs describe the influence of each on the overall process as observed during the 17 runs.

MELTING

The melting phase was conducted in a conventional manner for superalloys. The process was straightforward, involving induction heating in a ceramic crucible under vacuum. The crucibles and pouring lips used throughout were $ZrO_2$ and were replaced after every four runs. Although superheat is desirable from an atomization point of view to reduce surface tension, the amount of superheat was maintained fairly low, i.e., about Tm + 250°K. The charge was composed entirely of vacuum-induction melted and vacuum arc remelted stock, nominally 7.62 cm. in diameter. Two roots blowers, each 1600 cfm and each backed by a 400 cfm mechanical pump, provided the means for chamber evacuation. Vacuum levels throughout the study were held to about 20$\mu$ to 40$\mu$, with leakup rates on the

order of 60 μ/min. These rates were considered somewhat high and were attributed to leakage around the turbine sealing mechanism. An argon bleed was used successfully as a differential gas supply to ensure no air contamination into the chamber and, during operation, continuous $O_2$ analyzing showed no existence of $O_2$ >17 ppm. The seal is presently being redesigned to eliminate entirely any supporting need for argon.

POURING

The flow of liquid metal from the crucible to the atomizer was analyzed in detail during this report period. The purpose of this work was to guarantee that the liquid metal could be metered and controlled at any given rate and in such a manner that uniform liquid atomization occurred. A tundish assembly was used for receiving the molten charge from the crucible and metering it via bottom pouring onto the atomizer. Materials of construction were the same as those of the melting crucible and preheating to a given temperature was achieved by radiation. The initial location of the tundish and size of orifice were selected in a somewhat arbitrary manner. This location, relative to the atomizer, was based principally on noninterference with other components and ability to locate recording devices throughout the vicinity of the atomization. The free fall distance, therefore, became about 30 cm. Orifice size was selected on the basis of delivering approximately 151 g/sec to the atomizer, a rate that seemed reasonable from the standpoint of bulk quantities, turbine hp, and He mass flow requirements for quenching. Control over rate was attained by manually controlling the head of liquid metal in the tundish. Relating back to mass flowrate effects on atomization, control of ±10% was considered adequate for these purposes.

Torricelli's theorem, $q = \rho a \sqrt{2\,gh}$, states that the flowrate of the liquid issuing from an orifice is a function of the nozzle area and level of the liquid in the container. In the above equation, $\rho$, a, g, and h are the density, nozzle area, gravitational constant, and height of the liquid, respectively. During the experimental work, it was found that the equation gave reasonably good predictions for flow of liquid superalloys.

Transients that occurred during filling and emptying of the tundish were considered relative to the overall operation but were found to be of minor import since, after some experience with the pouring mechanism, it was found that these

transients could be held to a combined total of less than 14 sec. Figure 4 illustrates the typical time function of the two transients.

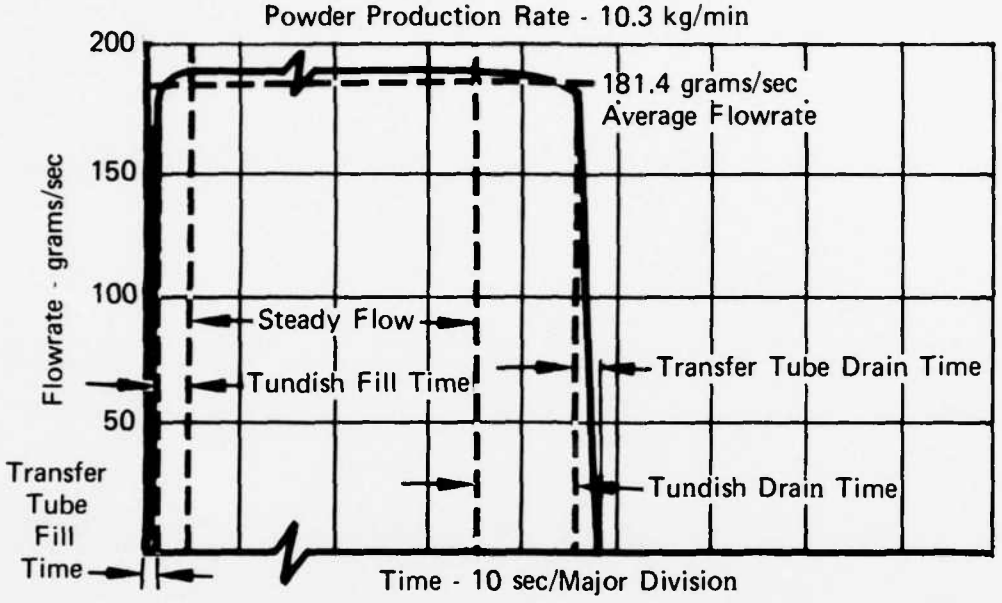


Figure 4. Liquid Metal Flowrate vs Time for RSR-18 Powder Run FD 98317

Level probes and total automation of the pouring rate were studied and results showed reasonable success. The probes were based on the use of ceramic-coated refractory metal rods spaced a short distance apart inside the tundish, enabling the operator to visually locate the level of the liquid and manually control the flowrate from the crucible. For the experimental work now being performed, this method has proved entirely satisfactory.

For extended periods of time, however, a better method will probably be needed, and the one being considered is control through the use of ceramic-coated refractory wires that are electrically conductive at melt temperatures. This means of control is simply an extension of the manual means, only the pour rate from the crucible would be controlled by an electric motor being signaled by one conducting probe as too low; the other, too high.

Stream stability from the tundish to the atomizer was recognized early in the testing to be a dominant factor in producing useful quantities of powder. In the first series of studies, high-speed cinematography revealed one flow characteristic that totally negated the ability of the atomizer to function properly. Figure 5 is a photo reproduced from one frame of a 400-frame/sec film. It

shows that the liquid stream had separated into large droplets prior to reaching the atomization surface. The effect was two-fold. One, it caused excessive splashing on the surface, and two, the periodic nature caused nonuniform atomization since each drop was seen to atomize separately from only a discreet portion of the surface.

Concurrent with continued testing in the AGT400,000 rig, model studies were started to define how best to circumvent this condition of noncontinuous flow. The model that was constructed is shown in figure 6. It consists of a liquid reservoir with metering valve, and a tundish-transfer tube assembly with interchangeable metering nozzles. Measurements of stream length were made with a standard scale and strobe unit. Water and mercury were used for the study.

Preliminary tests revealed that the location of the pouring stream could effect subsequent stability if the liquid were maintained at too low a level, i.e., ~1.25 cm. Pouring directly into the center of the transfer tube also produced instabilities and premature breakup, especially when the tube length was short.

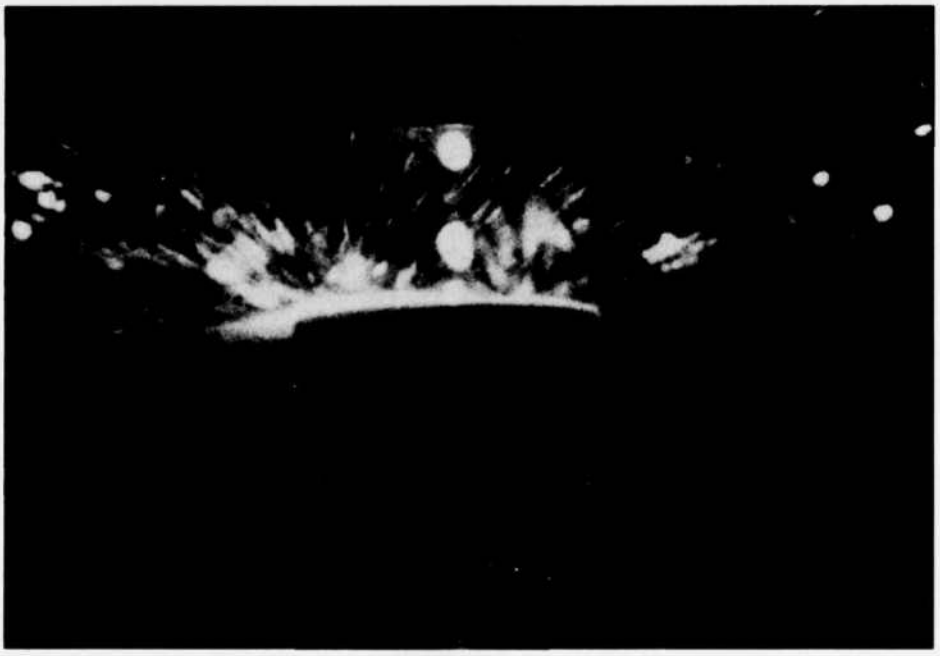

Figure 5. Characteristics of Atomization Under Unstable Stream Conditions FC 33518

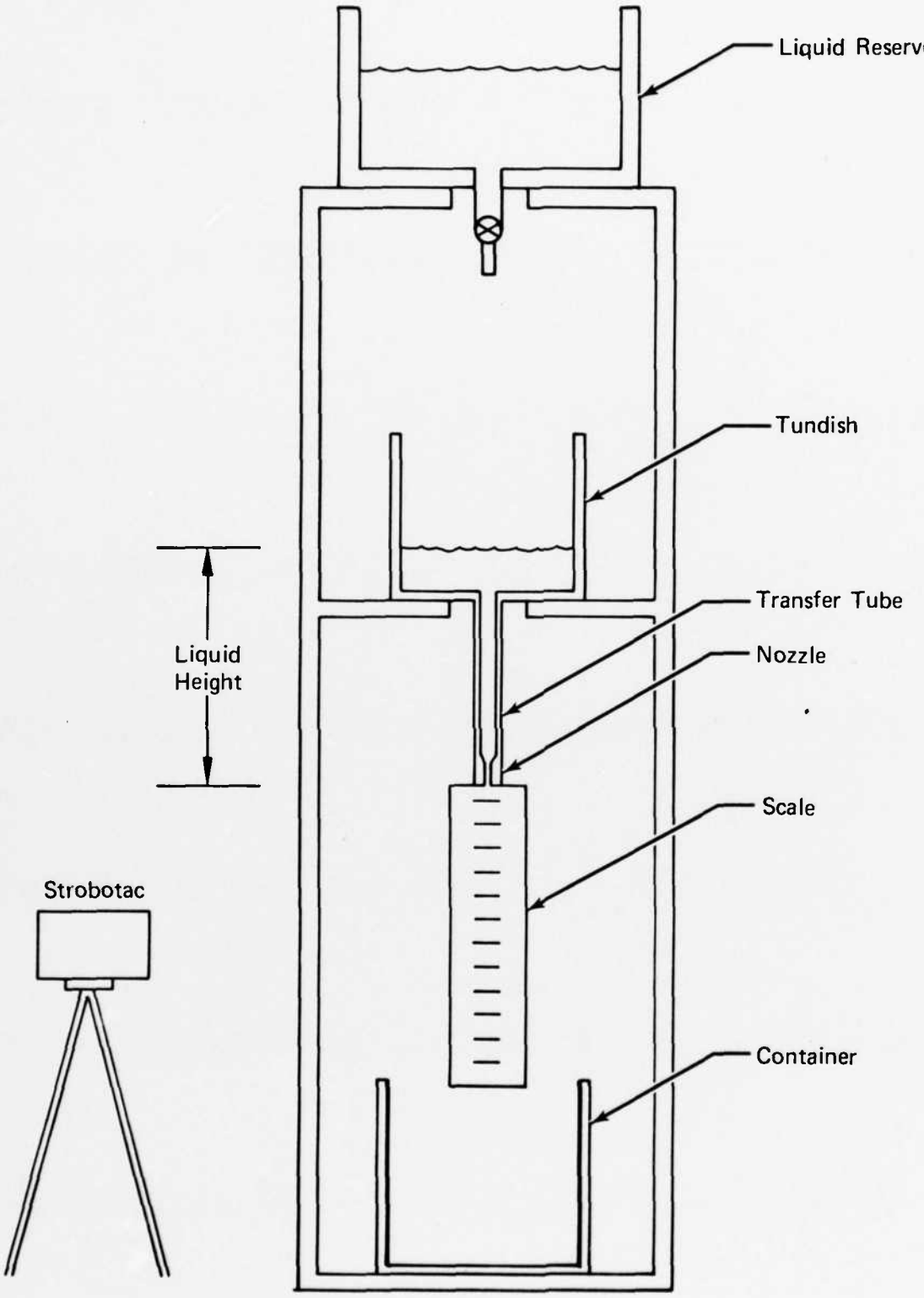


Figure 6. Schematic of Apparatus to Measure Liquid Stream Breakup Length

FD 98318

The length of a continuous stream from a nozzle can be expressed by the equation

$$L = Kv\left(\frac{d^3\rho}{\sigma}\right)^{1/2}$$

where

K = constant
v = stream velocity
d = nozzle diameter
$\rho$ = liquid density
$\sigma$ = surface tension

The principle underlying the above expression as it applies to a molten superalloy is that stream instability occurs because of high surface energy associated with high surface tension. Any disturbance of the stream during atomization can cause "varicose" breakup and subsequent rapid spheroidization. The opposing forces that assist in preventing stream breakup are viscous and inertia forces. However, for liquid metals, which typically have low viscosities (around 4-5.5 centipoise for nickel at 1895°K), only inertial forces play a role. Consequently, for a liquid metal stream, length prior to breakup can be increased only by increasing the velocity of the jet or by increasing nozzle diameter.

Low velocities are highly desirable for the process in order that erosion in the tundish metering nozzle is minimal, and, likewise, large nozzles mean higher than desired mass flowrates.

Returning to the expression for stable stream length, experimental studies determined a value of $\sim 3$ for K. The K values for water decreased slightly with decreasing head, but remained essentially unchanged for mercury. Calculating stable stream lengths for molten IN100 from these data showed that distances on the order of 8 cm, rather than 30 cm, were more proper if continuous flow to the atomizer was desired. The experimental data with water and mercury and observed and calculated stable stream lengths for liquid IN100 are shown in table 1. Also shown in the table are the velocity profiles associated with stable flow under these conditions. It can be seen that they are extremely low for the given conditions and, in all probability, would result in little, if any, nozzle erosion during actual generation.

TABLE 1. LIQUID STREAM BREAKUP LENGTH EXPERIMENTAL VALUES ($K = L/\nu\ (d^3 \times \rho/\sigma)^{1/2}$)

| Liquid | d, cm | h, cm | $\nu$, cm/sec | $\rho$, g/cm | $\sigma$, dynes/cm | L, cm | K |
|---|---|---|---|---|---|---|---|
| $H_2O$ | 0.32 | 6 | 108 | 1 | 70 | 10 | 4.3 |
| $H_2O$ | 0.32 | 13 | 160 | 1 | 70 | 11.5 | 3.3 |
| $H_2O$ | 0.32 | 20 | 200 | 1 | 70 | 13 | 3.0 |
| $H_2O$ | 0.40 | 6 | 108 | 1 | 70 | 13 | 4.0 |
| $H_2O$ | 0.40 | 13 | 160 | 1 | 70 | 18 | 3.7 |
| $H_2O$ | 0.40 | 20 | 200 | 1 | 70 | 19 | 3.1 |
| Hg | 0.32 | 6 | 108 | 13.6 | 435 | 9 | 2.6 |
| Hg | 0.32 | 13 | 160 | 13.6 | 435 | 13 | 2.5 |
| Hg | 0.32 | 20 | 200 | 13.6 | 435 | 15 | 2.3 |
| Hg | 0.40 | 6 | 108 | 13.6 | 435 | 13 | 2.7 |
| Hg | 0.40 | 13 | 160 | 13.6 | 435 | 19 | 2.6 |
| Hg | 0.40 | 20 | 200 | 13.6 | 435 | 27 | 3.0 |
| IN100 | 0.32 | 6 | 108 | 7.85 | 1700 | - | - |
| IN100 | 0.32 | 13 | 160 | 7.85 | 1700 | - | - |
| IN100 | 0.32 | 20 | 200 | 7.85 | 1700 | 7.5 | 3.0 |
| IN100 | 0.40 | 6 | 108 | 7.85 | 1700 | - | - |
| IN100 | 0.40 | 13 | 160 | 7.85 | 1700 | - | - |
| IN100 | 0.40 | 20 | 200 | 7.85 | 1700 | >7.5 | - |

CALCULATED STREAM LENGTH FOR IN100 (K = 3)

| d, cm | h, cm | L, cm |
|---|---|---|
| 0.32 | 6 | 4 |
| 0.32 | 13 | 6 |
| 0.32 | 20 | 7.5 |
| 0.40 | 6 | 5.5 |
| 0.40 | 13 | 8 |
| 0.40 | 20 | 10 |

The data reported above were used to modify the AGT400,000 tundish assembly from one having a drop length to the atomizer of 30 cm to one of about 8 cm. For expediency, the tundish was modified to include a transfer tube located in the tundish base such that the metering nozzle could be relocated without

extensive rework of the basic device. The present arrangement is shown in figure 7. This scheme has been used for the past 8 runs and, in every case, stream continuity to the atomizer has been achieved. Figure 8 shows the typical stream appearance to the atomizer with this modified system. If desirable in the future, further changes, such as locating the tundish metering nozzle immediately above the atomizer, can be made. Such has not been done now since the present method works well, and poses the least interference to the recording systems being used for data analysis.

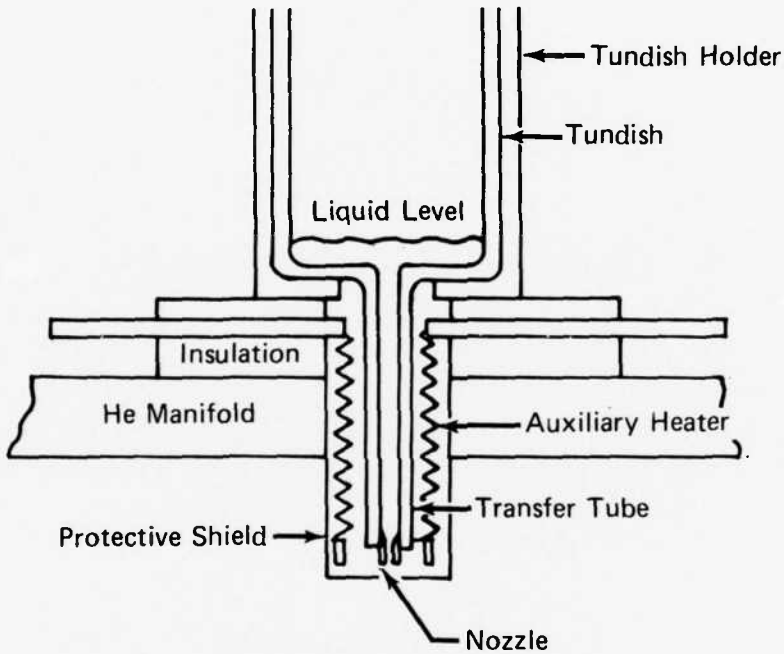


Figure 7. Schematic of Metering Tundish, Transfer Tube, and Nozzle System for Continuous Stream FD 98319

ATOMIZATION

The experimental runs made during this period were conducted principally to check out the structural integrity of the rig, stability characteristics, and interaction effects among the three major operations - pouring, atomization, and quenching. The atomization speed range was on the low end of the scale that is being considered for operation and was typically in the range of 5,000 to 16,000 rpm. The upper limit of 16,000 rpm was an equipment limitation in the form of a transient temperature condition in the turbine bearings. The cause for this was the use of an oil mist lubrication system that limited the amount of oil injected into the bearing compartments. An oil jet system has

been designed and is presently being implemented into the turbine drive system to circumvent this problem. This oil limitation likewisc caused a speed decay during operation that hindered the subsequent analysis of metal powder yield as a function of speed.

Nevertheless, atomization studies proceeded smoothly in areas of atomizing surface requirements and interaction effects.

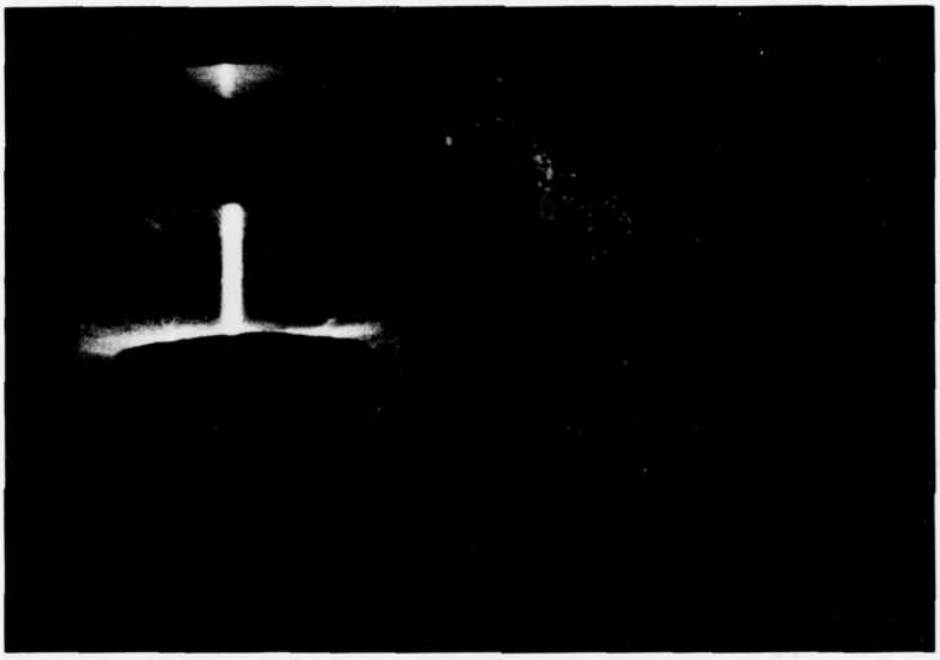

Figure 8. Characteristics of Atomization Under Steady-Stream Conditions FD 33521

The surface conditions that are being considered in this program include conditions for which the surface is either above $T_m$, forming no skull and operating in a noncoupling mode, or below $T_m$, forming a skull and atomizing from a coupled surface. Each has its advantage. Surfaces operating above $T_m$ can take ready advantage of superheat and entirely eliminate the need to design imbalance characteristics into the rotor assembly. Surfaces operating below $T_m$ operate as wetted surfaces and, according to most published reports, produce finer particles. For studies of surfaces operating above $T_m$, zirconia-coated tantalum was used. The assembly was insulated from the rotor mechanism and was brought to temperature by contact with the metal stream itself. Studies of surfaces operating below $T_m$ were conducted with water-cooled copper.

Of the 17 runs made, the first 6 were run with stream instability caused by the condition of pouring. In each of these cases, atomization amounted to about 50% of the poured weight, while splashing accounted for the balance. Subsequent film analyses, such as those shown in figures 5 and 8, showed clearly that the molten metal that did atomize did so in independent fashion and in a manner leading to a condition that will be termed "channeling," a state whereby the liquid mass did not flow uniformly to the atomizer rim but rather followed a path leading to atomization only over a very small portion of the periphery. Such a condition, even though it yielded useful amounts of powder, was considered totally unsatisfactory because of its unstable, unpredictable nature.

Six of the seventeen runs were made with zirconia-coated tantalum, three of these prior to stabilization of the liquid metal stream. In all cases, surface temperature above $T_m$ was achieved in about 1 to 2 sec. Where stream instability occurred, splashing and lack of control were common. Under conditions of stream stability, atomization took place uniformly and free of skull. The attachment means used to hold the disk to the rotor proved to be unreliable, however. Initially, the tantalum was spot welded around the periphery to a second tantalum holddown ring. These welds failed at speeds in excess of 10,000 rpm and a second method involving rivets was employed. This method was no better. At present, the entire assembly is being redesigned to provide a fail-safe holddown mechanism.

Water-cooled copper surfaces, which were used in the balance of the runs, proved to be most interesting. At the start of the program, it was known that a particular heat balance would be required so that heat lost to the water coolant would not set up an uncontrollable skull formation. The first runs with copper were made to determine the extent of skull buildup under conditions of no heat balance and also to provide data necessary to define heat flux on the disk. The typical skull formation during these runs is shown in figure 9. What is evident is continuous growth during running and severe channelling of the liquid stream to the periphery. Imbalance loads as high as 900 g-cm, an extremely high amount, were measured from skulls of this type but were not detrimental to the rotor assembly for the speeds considered.

The preliminary heat flux profile on the copper surface is shown in figure 10, and is translated to total heat lost to the atomizer in figure 11. This

amount represents about 16% of total heat in the systems. Calculating requirements to hold a stable skull from these data indicated that copper, because of its high conductivity, was not a reasonable choice for the atomizer surface. Rather, a material of low conductivity (the alloy itself, perhaps) was more desirable and could be designed into a configuration whereby a stable skull could be maintained.

For simplicity at this time, the copper surface was insulated with about 0.25 mm of zirconia and the runs repeated. The results were dramatic in improvement. What was found was the ability to stabilize the skull at a thickness around 1.27 mm for the flowrates considered. During operation in this mode, coupling (wetting) to the skull was attained, channelling appeared minimal, and atomization proceeded uniformly around the periphery. No instability was observed from start of run to completion. The typical skull for these conditions is shown in figure 12. The previous figure 8, which shows a stable stream occurrence, was taken immediately upon achieving constant liquid head in the tundish on one run using insulated copper. Figure 13 is a frame from the same film taken immediately before the head of liquid metal started to decrease at the end of the run. No differences can be observed. No imbalance resulted during this operation.

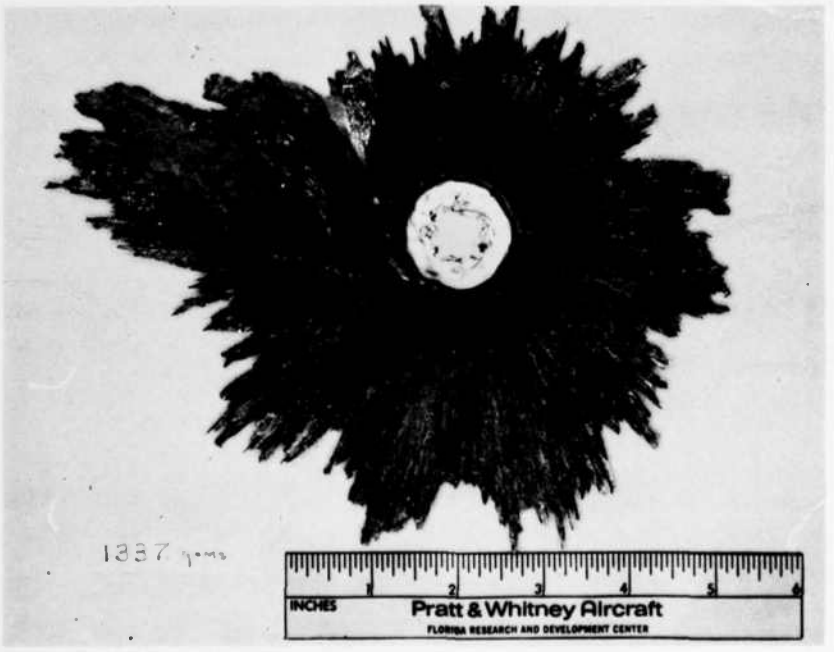


Figure 9. Typical Skull Buildup Without Heat Balance, RSR Run No. 14 FAL 37557

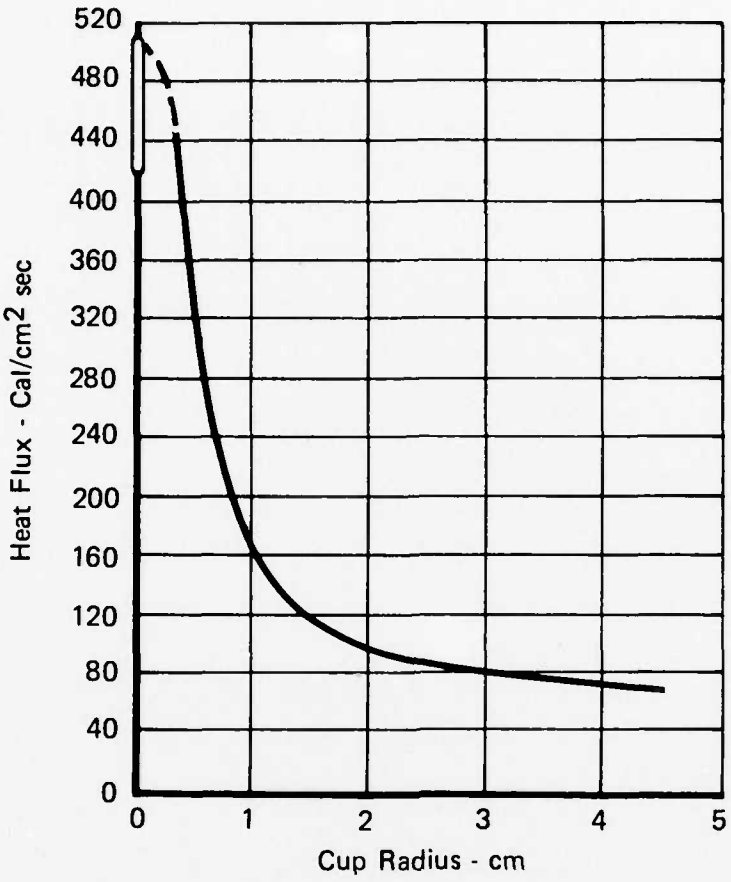


Figure 10. Liquid Metal Heat Fluxes to Skull-Forming Atomizers, 10,000-16,000 rpm FD 98337

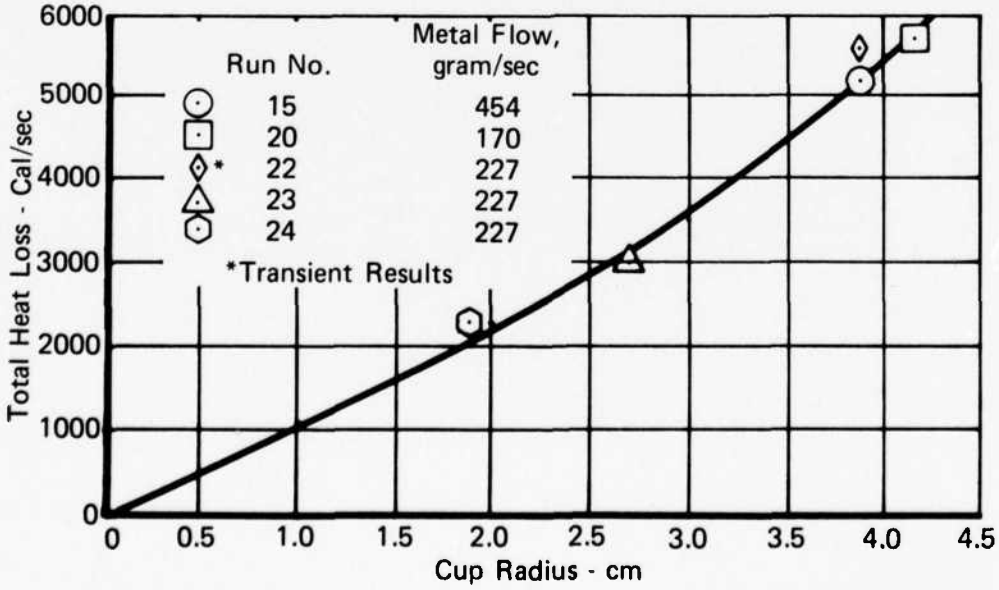


Figure 11. Liquid Metal Heat Losses to Skull-Forming Atomizers, 10,000-16,000 rpm FD 98338

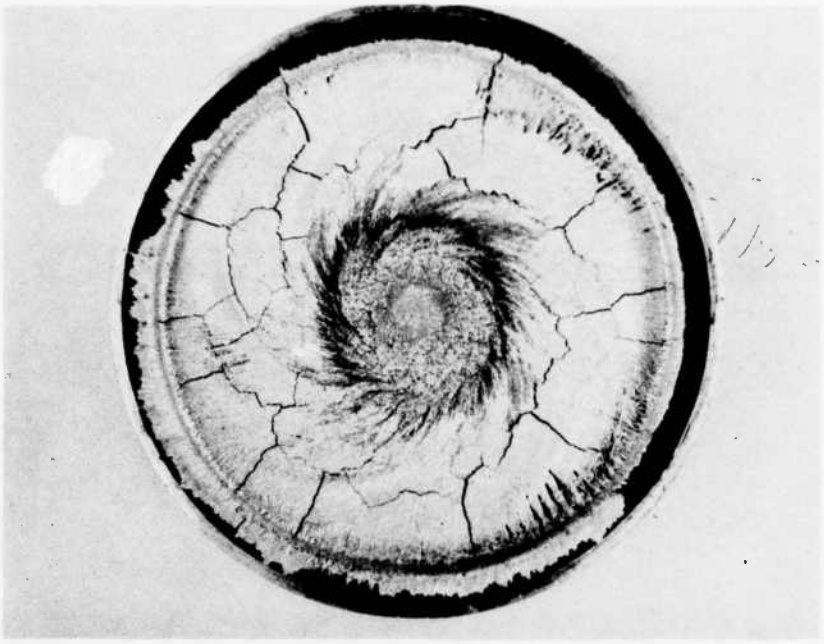

Figure 12. Typical Skull With Heat Balance

Figure 13. Characteristics of Atomization Under Steady-Stream Conditions - T + 60 seconds FC 33523

It should be pointed out that the runs to date are insufficient to state that even a near optimum condition has been identified for surface control on the particle generator. Study of heat flux profiles as a function of speed, surface area, metal flowrate, and superheat will be continued, and iterative analyses will be used in the next report period to provide a degree of refinement to this present data.

Where stable operation of the device was achieved, with the exception of the previously noted speed decay occurrence, yield characteristics were determined for comparison to the data calculated for rotary atomization (figure 2). These results are shown in figure 14 and are all from runs made with a 7.62 cm diameter disk surface. Agreement with the predicted data appears good. It will be necessary, of course, to significantly enlarge the data base prior to reaching basic conclusions relative to the atomizer and its handling of the superalloy material.

QUENCHING

The AGT400000 device is constructed in a manner to provide He mass flowrates up to 0.9 kg/sec and to distribute the gas according to an analytically defined cross flow pattern. This actual setup in the rig uses three annular gas nozzles for this purpose, each sized to maintain a high $\Delta T$ between the He environment and the cooling particles. These nozzles can be used simultaneously, singly, or in any desired combination. The analytically predicted heat release to the He atmosphere is shown in figure 15. It is independent of particle size as long as all the particles reach the same final temperature. Particle size, trajectory, and cooling gas distribution establish the heat release profiles; the smaller the particle diameter, the closer to the atomizer that the heat is released. Figure 16 illustrates this principle.

In the series of runs conducted during this period, the He mass flowrates were varied from a static environment (0.129 $MN/m^2$) to 0.9 kg/sec. The bulk of these runs were made at 0.23 kg/sec. Although it was desired to use the higher mass flowrates for maximum quench effect, it was found during the initial runs and from 1/3 model studies that a turbulent condition is caused by the innermost nozzle that can change the stability characteristics of the operation. This turbulent condition can be eliminated by introducing a shield between the generator and the nozzle. This was not done because it would compromise the ability to

analyze particle generation (no field of vision). However, it was felt that until a better defined state of particle generation was attained, maximum quenching was unnecessary. Further, the analytical prediction of effect of high gas flow predicts that cooling rates increase by less than a factor of 2, and in studies of resulting microstructures, which are discussed subsequently, desired rates were being attained with the system operating as described.

Thermal probes installed in the device to record local temperature transients that could confirm the conditions expressed in figures 15 and 16 have not been entirely successful. This was due to difficulty in locating the probes where meaningful data could be obtained while, at the same time, where they would not interfere with the atomizing itself. Infrared is being considered presently as an alternative method.

The helium being used is Bureau of Mines Grade A quality. It is certified at less than 10 ppm $O_2$ and less than 30 ppm moisture. At no time during operation did it appear that the gas quench could contribute to contamination.

In addition to the study of cross-flow nozzle assemblies, further attention is being paid to the use of more advanced delivery concepts. The particular concept being considered is the use of a swirl jet, which by centrifugal force can set up an extremely sharp temperature transition from the particle generator to the quench environment without imposing difficulties in construction. It must be anticipated that the particles leaving the atomizing disk will consist of a range of sizes traveling at a range of speeds at, generally, a small angle to the plane of the disk.

On this basis, it follows that the cross flow of the gas at any point must be such that the heat absorbed from the particles does not cause a large increase in the gas temperature if the cooling rate of the particles is not to be impaired. Conversely, if the temperature rise in the gas is small, increasing the cross flow would have a minor effect on the cooling rate, except as it affects the relative velocity between the particles and the gas and, thereby, the heat transfer coefficient.

| Run | RPM | RPM Avg | Flow Rate grams/sec | Weight % Powder <177μ | Weight % Powder <105μ |
|---|---|---|---|---|---|
| 14 | 13K-10K | 11.5K | 136.1 | 39.6 | 10.1 |
| 16 | 12.5K | 12.5K | 362.9 | 32.5 | 10.5 |
| 18 | 14.3K-10K | 12K | 181.4 | 36 | 9 |
| 19 | 16.5K-13.5K | 14.5K | 181.4 | 58 | 25 |
| 20 | 16.2K-14.6K | 15K | 181.4 | 61 | 24.4 |
| 21 | 16K-10K-14.5K | 13K | 181.4 | 41.3 | 11.2 |

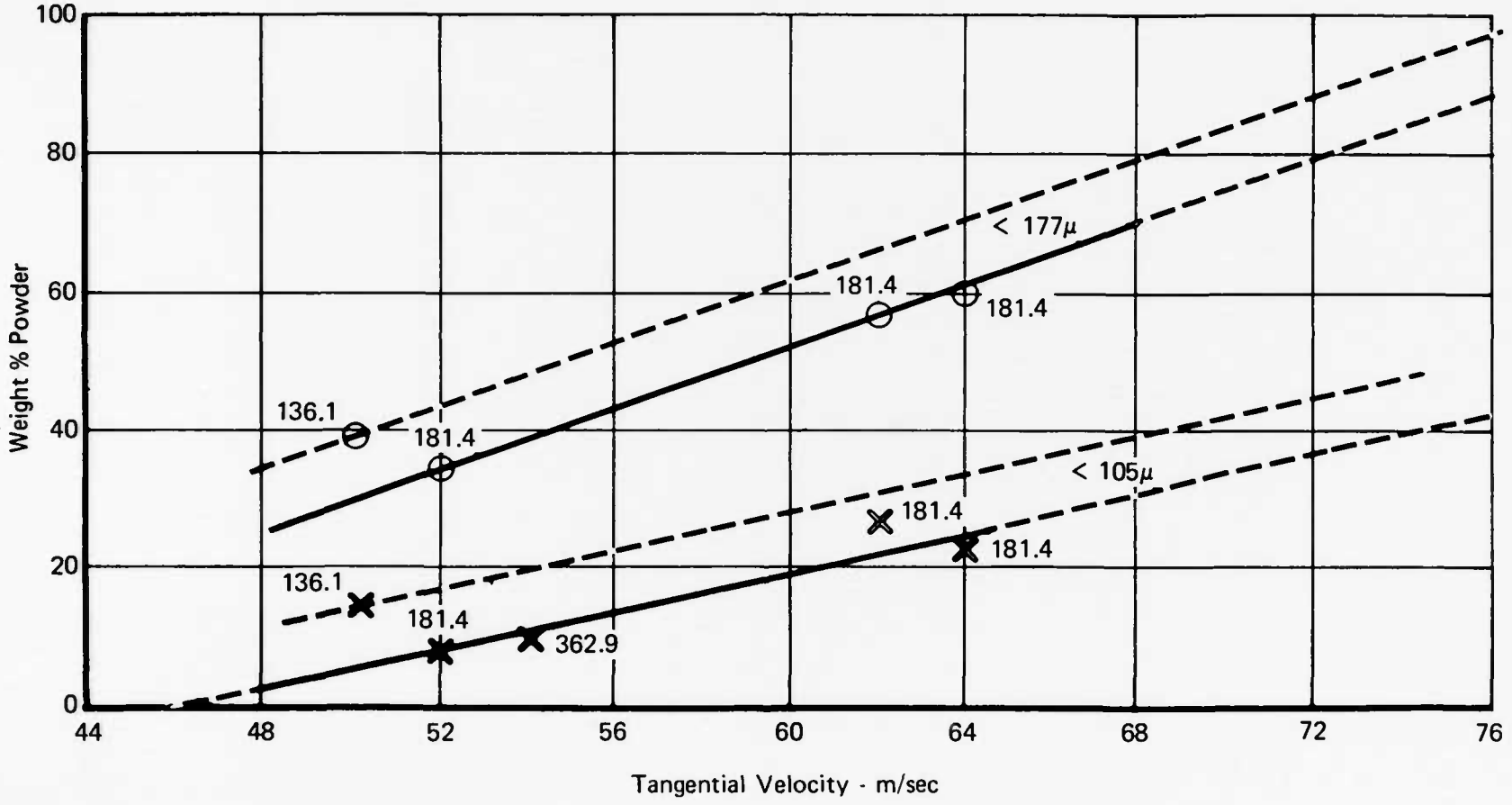


Figure 14. Weight Percent of Powder for Two Size Fractions

FD 98320

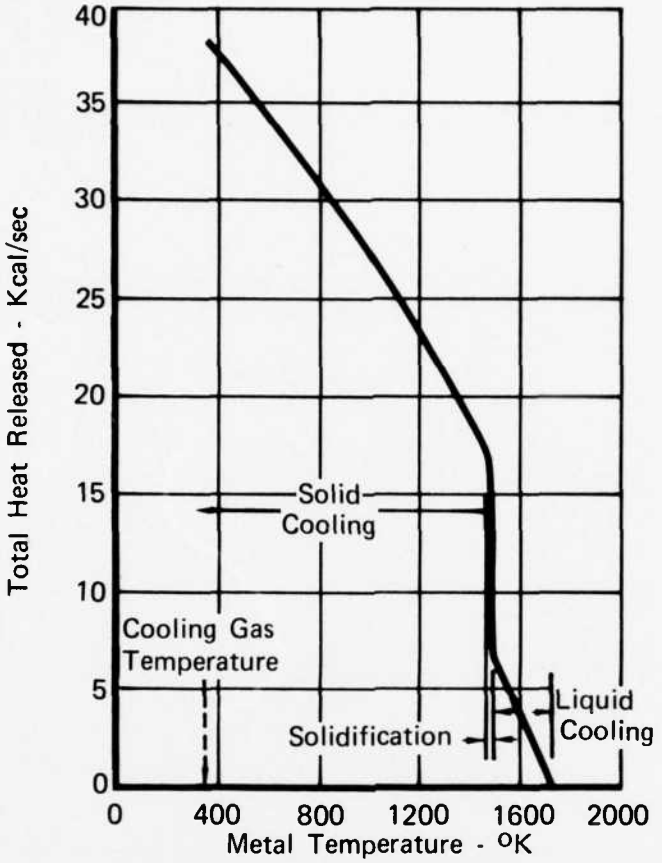


Figure 15. Total Heat Rejected to Helium Atmosphere at 350°K (151.2 grams/sec Superheated Liquid IN100) FD 98321

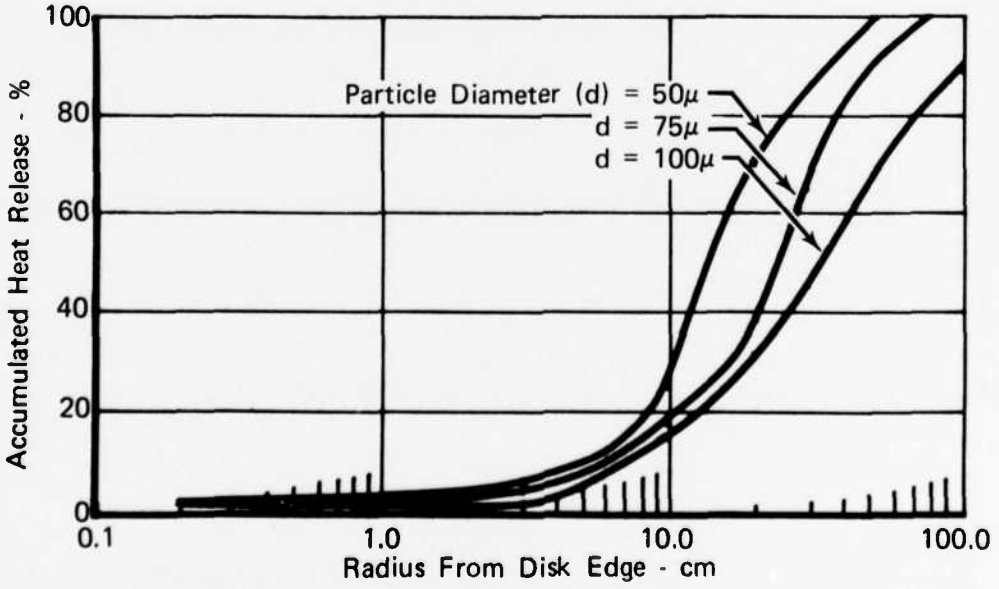


Figure 16. IN100 Particle Heat Release Profiles FD 98322

The particle density and the heat released decreases as the distance from the rim of the atomizing disk increases:

$$D = k/Vr$$

Where D = particle density
V = radial particle velocity
r = radius
k = constant

For particles leaving the atomizing disk tangentially, the radial component of velocity tends to increase as the trajectory becomes more nearly parallel to a radius, while aerodynamic drag decreases the velocity. Typically, the radial component of velocity is at a maximum a few inches from the rim of the disk. The particle density and the radial component of velocity for conditions assumed to be of interest are shown in figure 17.

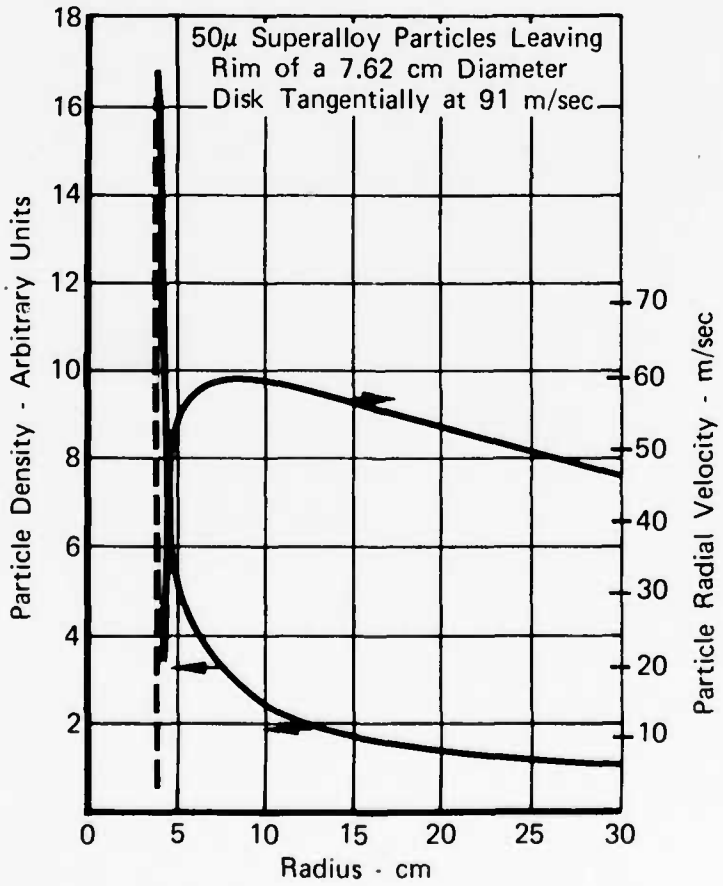


Figure 17. Particle Density FD 98323

The rapid decrease in particle density with increasing radius suggests that it might be advantageous to extend the hot environment outward from the atomizing disk and terminate it in an abrupt transition to the quenching gas jet. In this way, the lower particle density would lower the temperature rise of the quenching gas. Such an extended hot region would necessitate bounding its surface by opaque, insulated walls; otherwise, heat loss by radiation and convection would be prohibitive. It would also be required to provide a window through which the particles could pass into the quenching gas jet. Heat loss by convection would need to be restricted so that the temperature of the hot environment could be maintained and the hot gas would not dilute the cold quenching gas significantly. Because the velocity of the quenching gas is high in order to remove the heat liberated by the particles, a tendency toward hot and cold gas mixing is possible and is believed to be proportional to the shear between the hot and cold masses.

This tendency for mixing can be counteracted by centrifugal forces acting on the density gradient in the gases, which is associated with the temperature gradient. A swirling jet of the quenching gas concentric with the hot region can provide the high centrifugal accelerations at the aperture. Initial calculations estimate that an effective gas swirl jet would have a tangential component of velocity in the range of 60 to 300 m/sec and an axial component sufficient to remove the heat liberated by the particles with a small temperature rise in the gas. Centrifugal accelerations of 1600 to 62,000g's would exist for apertures 30 cm to 46 cm in diameter.

A model apparatus has been constructed for studying the effect of centrifugal force on the separation of gases of varying density despite shear between the gases. The model is shown schematically in figure 18.

Rather than creating a density gradient by means of a temperature gradient as in the present apparatus, the model employs gases of different molecular weights. Helium is being used to simulate the hot gas, and air to simulate the cold gas. Vanes in the airflow impart swirl to the air jet, with conservation of angular momentum causing tangential velocity to increase as the aperture is approached.

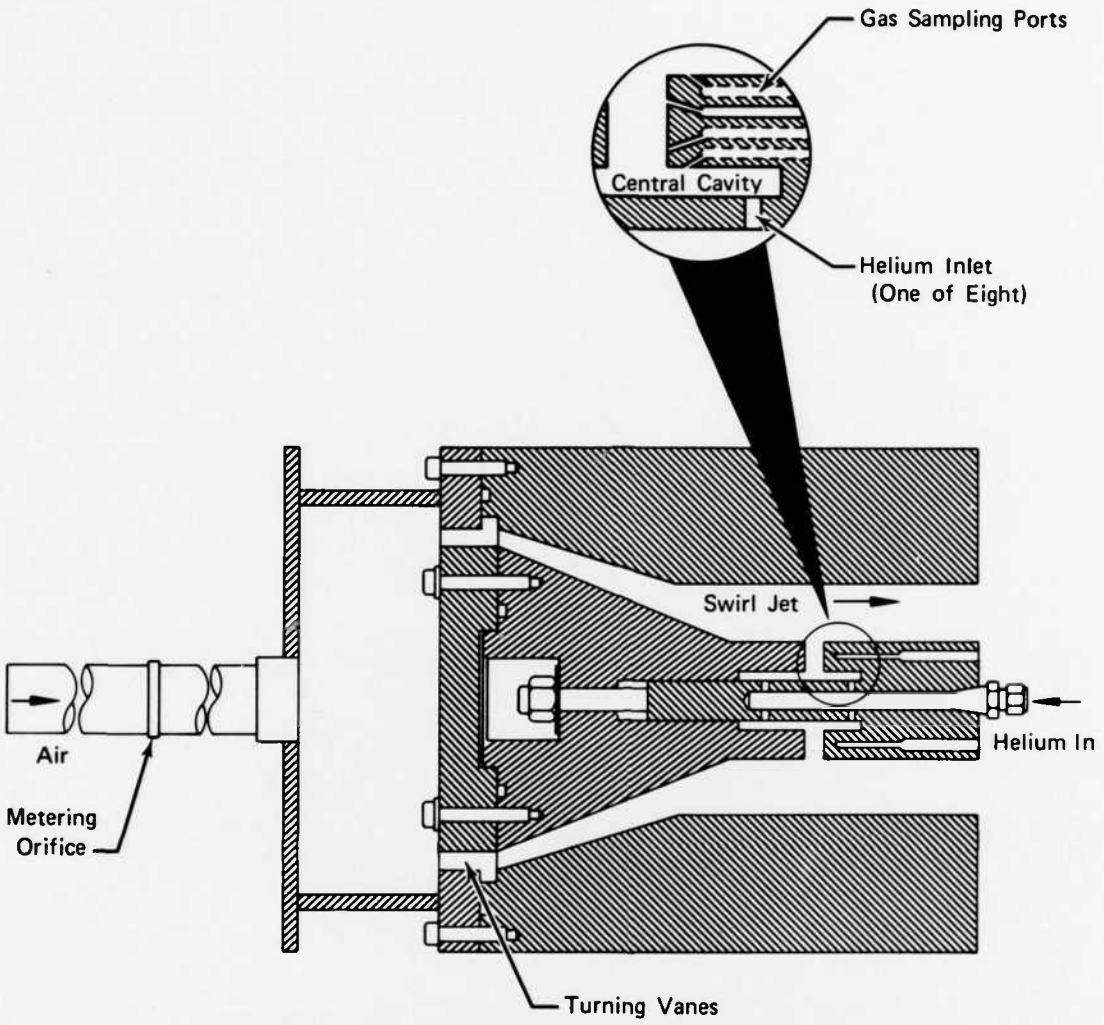


Figure 18. Swirl Flow Model FD 98324

A computer program that assumes compressible, inviscid flow has been used to calculate gas velocity, static pressure, and static temperature as a function of position for a variety of swirling jets. The jets were assumed to be generated by turning vanes followed by a transition section that could be either a nozzle or a diffuser. A subroutine that was adapted from the program discussed earlier in the report calculated the trajectory and cooling rates of metal particles considering the effect of centrifugal forces on the particles.

The results of these calculations indicated that swirl jets produce equivalent cooling rates to straight cross-flow cooling with significantly reduced mass flow

of quenching gas or higher cooling rates with equivalent flows of gas. This is illustrated in figures 19 and 20 for a typical set of conditions:

| | |
|---|---|
| Alloy - | IN100 |
| Flowrate of metal - | 151 grams/sec |
| Initial temperature of metal - | 1811°K |
| Particle diameter - | 50 microns |
| Initial radial velocity of particles - | 51 m/sec |
| Initial tangential velocity of particles - | 1.83 m/sec |
| Mass flow of helium - | 0.9 kg/sec |
| Total pressure - | 1 atmosphere |
| Total temperature - | 350°K |
| Vane angle - | 1.25 radians |
| Outer radius at vanes - | 73.79 cm |
| Inner radius at vanes - | 68.58 cm |
| Outer radius at aperture - | 35.56 cm |
| Inner radius at aperture- | 22.86 cm |

The tangential velocity for typical conditions is the dominant factor in determining the relative velocity between the particle and quenching gas. In the swirl jet model, this velocity exceeds the axial component by a factor of seven. Since the cooling rate increases with relative velocity, the mass flow for straight flow would have to exceed that of the swirl jet by nearly that factor to produce equivalent cooling rates. The cooling rate as a function of relative velocity is shown in figure 21. Although the rate increased continuously with relative velocity, the increase was not as rapid as the increase in kinetic energy of the jet (except at velocities below 91-122 m/sec). Figure 22 shows the relationship between the incremental increase in cooling rate per unit of kinetic energy of the jet and the relative velocity.

## COLLECTION

The AGT400000 rig is equipped with two collectors, each of which can be sealed independently from the unit itself for inert transfer to any subsequent operation. One of the collectors is located immediately below the atomization chamber. The second is located below an appendage cyclone separator. Ducting to and sizing of the cyclone device was based on 0.9 kg/sec He gas exhaust velocities being above the critical velocity for fine particle motions.

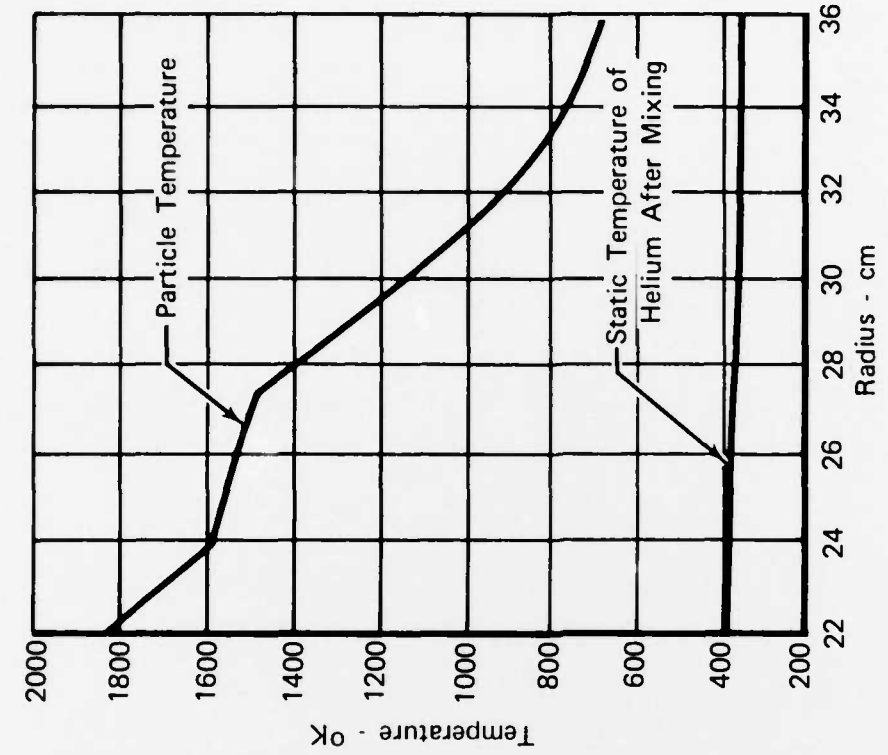


Figure 20. Particle Cooling in a Swirl Jet

FD 98326

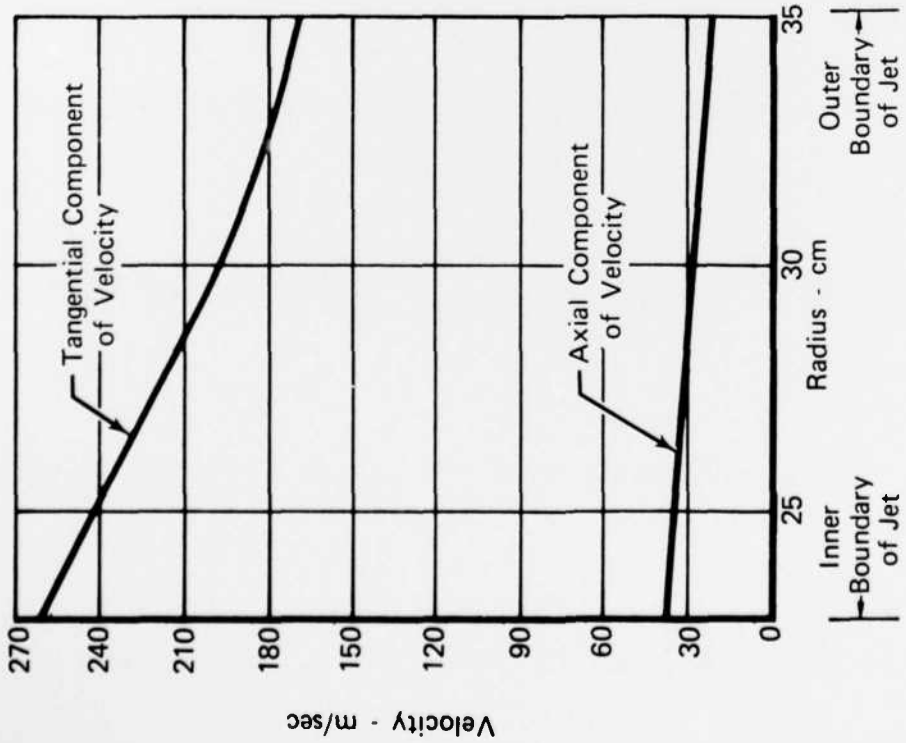


Figure 19. Typical Swirl Jet

FD 98325

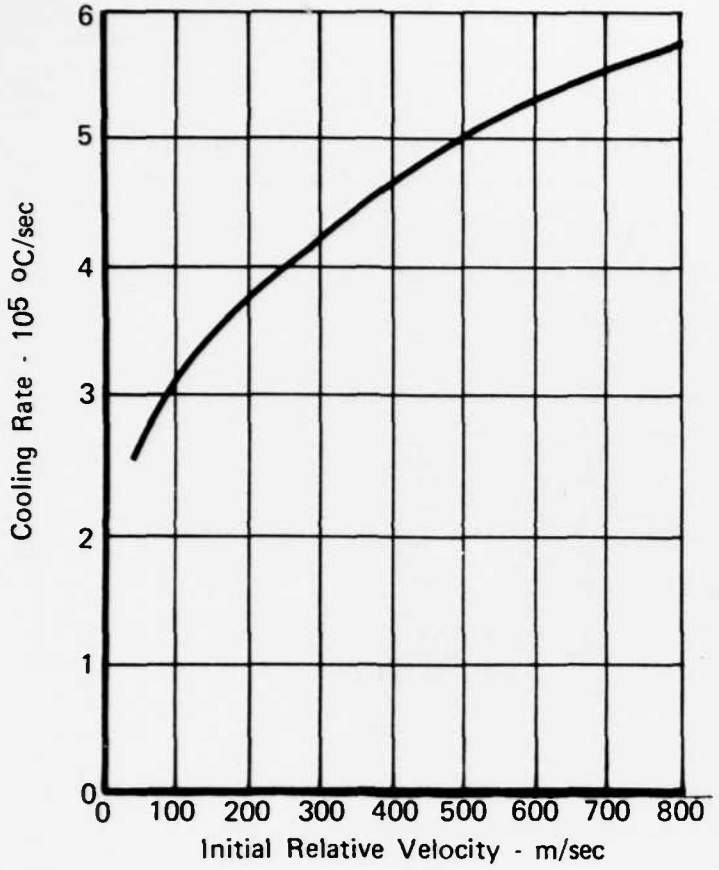


Figure 21. Effect of Realtive Velocity on the Cooling Rate FD 98327

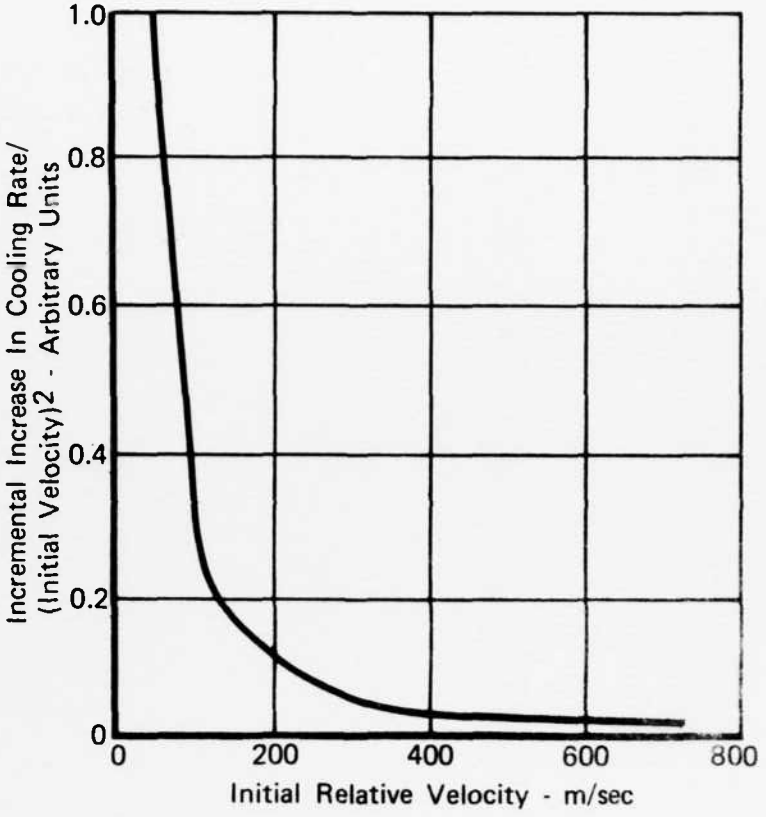


Figure 22. Incremental Increase in Cooling Rate as a Function of Relative Velocity FD 98328

The collectors appear to operate completely satisfactorily. No difficulties have been encountered in any form of environmental contamination. The number of runs made is still low, however, and a degree of temperance must be exercised in this judgment. Transfer equipment to accept the inertly contained powder is presently being fabricated for future work. At present, the powder is being handled in the ambient atmosphere following its production.

## SECTION III
## MATERIAL EVALUATION

The powdered material produced in each run is being evaluated with respect to cooling rates attained, effect of such rates on microstructures, and product acceptability relative to present quality standards for superalloy powder.

The typical appearance of the alloy powder is shown in figure 23. The material is spherical and free from aggregate formation like that which occurs when molten particles impact one another. The surface structure becomes progressively finer with decreasing particle size, indicative of faster cooling. Flake can be seen as part of the collection and the extent was found to vary from run to run, depending on the atomization speed, operational stability, gas flow-rate, etc. It is attributed to coarse particles impacting with the chamber prior to solidification and, subsequently, breaking up into a variety of sizes. Once desired operating conditions are attained, it is reasonable to believe that such occurrences will be negated.

Dendrite arm spacing has been used by numerous investigators as a means to experimentally determine cooling rate. This relationship is shown in figure 24. Accordingly, these same measurements are being made for the powder material produced in this program. These measurements, by necessity, require a high degree of precision since minor errors can lead to substantial misjudgment relative to true cooling rate. The method used in the present work is based entirely on metallurgical replication procedures and subsequent analysis by electron microscopy. Reasonably large sample sizes, (i.e., on the order of 50 independent samples per run) are also being used to determine whether any significant differences can be detected from particle to particle. Further, because of geometric consideration, measurements are being confined to those dendrites in which the central arm exhibits secondary arms on both sides and where the dendrite length exceeds the central arm width by at least a factor of 5.

The cooling rates determined by this method for the IN100 alloy are shown in figure 25 and are also compared to the analytically predicted capability of the AGT400,000 device. The data points shown are representative of samples for which the gas quench was operating at 50% of capacity or greater. The correlation appears reasonably accurate and confirms that cooling rates in excess of $10^5$°C/sec can be achieved when particle diameters are less than $\sim 100\mu$.

Typic

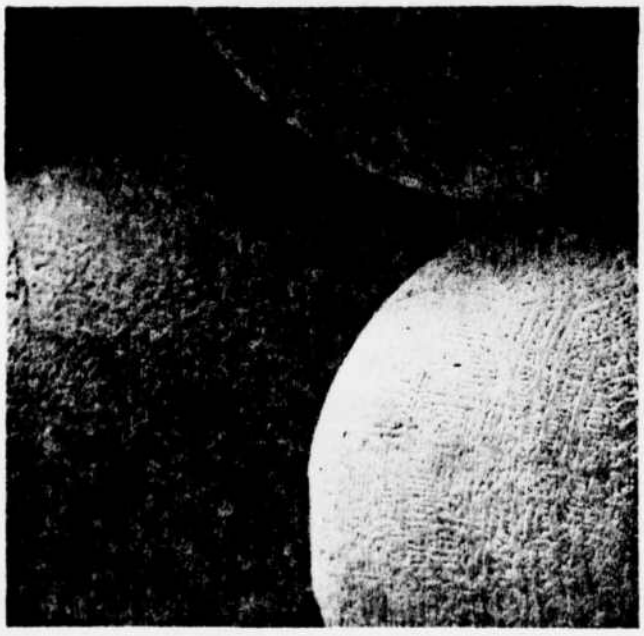

105$\mu$ - 177$\mu$ Particles

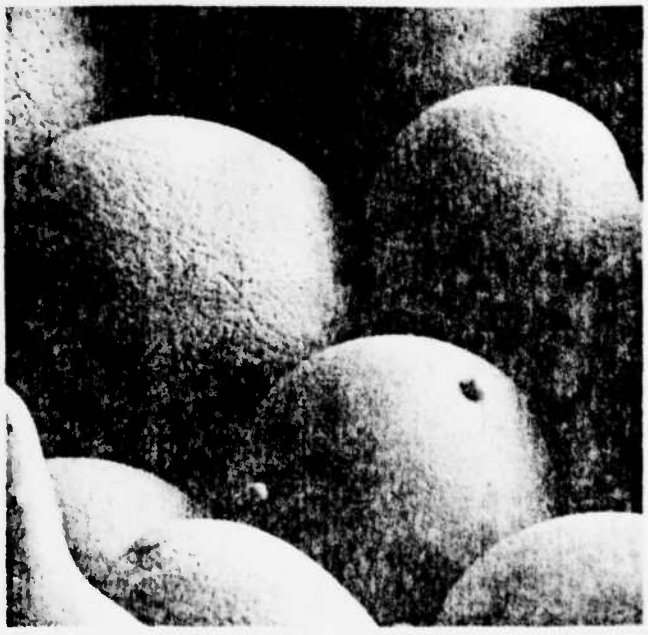

65$\mu$ - 105$\mu$ Particles

Lower Photos All 500X

Figure 23. Surface Appearance of IN100 Alloy Powder

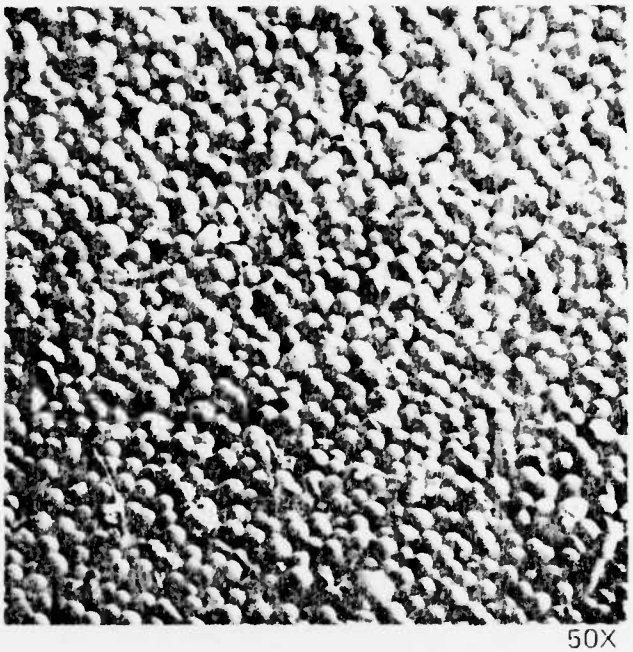

50X

Typical Sample

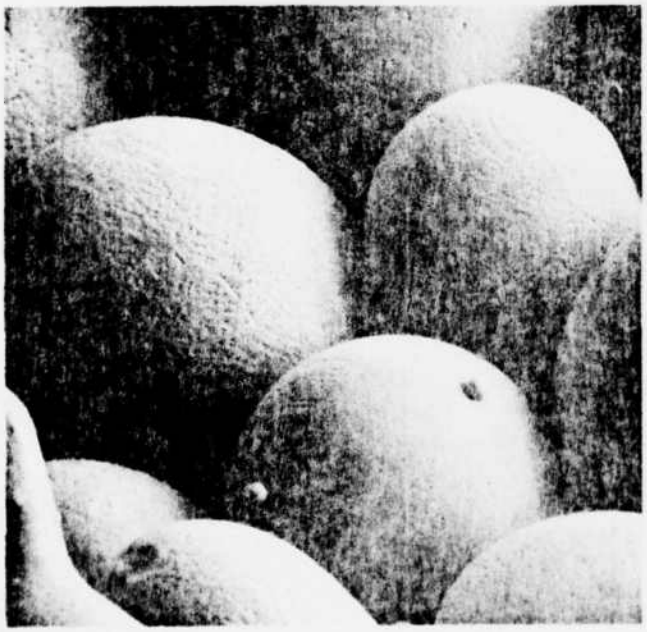

65$\mu$ - 105$\mu$ Particles

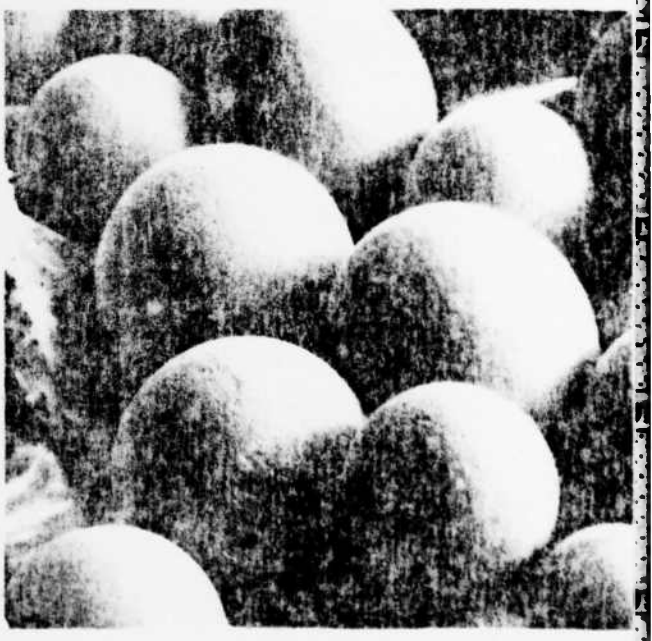

45$\mu$ - 65$\mu$ Particles

Alloy Powder

2

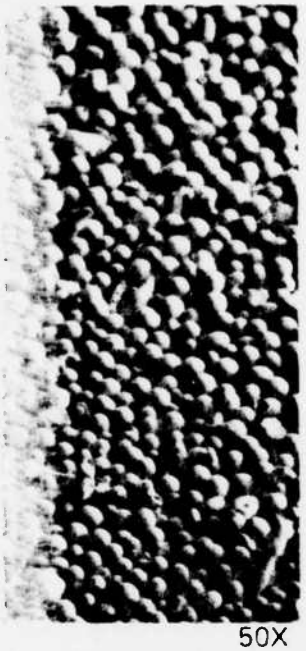

50X

mple

45μ - 65μ Particles

<45μ Particles

FD 98339

3

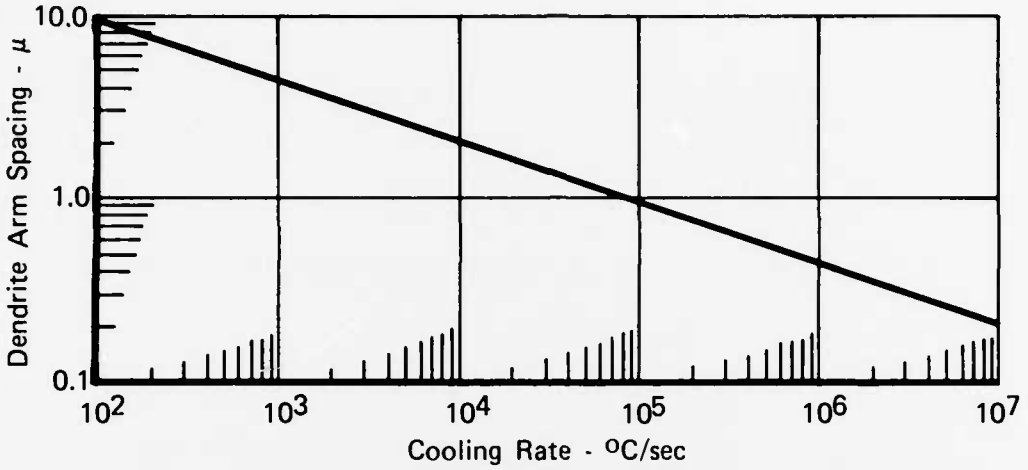


Based Upon Joly, P. A. and R. Mehrabian, "Complex Alloy Powders Produced by Different Atomization Techniques: Relationship Between Heat Flow and Structure," Journal of Materials Sci., 9, 1974, p. 1449
And
Matyja, H. et al, "The Effect of Cooling Rate on the Dendrite Spacing in Splat-Cooled Aluminum Alloys," Journal of the Inst. of Metals, Vol 96, 1968, p. 32

Figure 24. Cooling Rates as a Function of Dendrite Arm Spacing FD 98341

The typical microstructures revealed during this effort are shown in figure 26 and are being used in conjunction with electron microprobe and X-ray studies to determine what effect fast cooling had achieved over conventional processing. The study is far from complete at this time; however, the results to date from powder exhibiting cooling rates greater than $10^5$°C/sec show that suppression of the secondary $\gamma'$ phase has been achieved. Eutectic formations and the like are, naturally, nonexistent. A significant, but not complete, suppression of a carbide phase has also been achieved, presently being detected only in the surface replicas used for dendrite arm spacing measurements. Chemical segregation studies by elemental X-ray mapping showed no preferential conditions. Composition of the powder did not vary with change in particle size.

Product quality has been analyzed in a somewhat casual manner to date. The reasons for this are two-fold. First, the existing capability for handling the powders involves breaking to an ambient environment, rather than maintaining the inert atmosphere under which the powder was produced. Second, many of the runs were made under conditions where operational instability of the rig was known to affect the quality of yield.

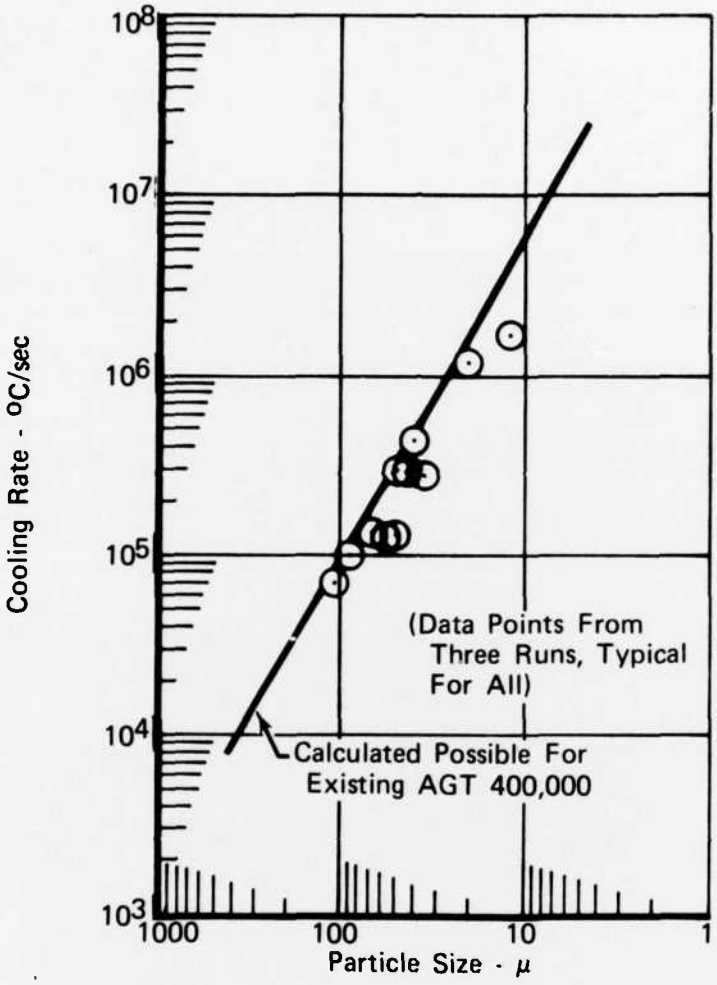


Figure 25. Experimentally Determined Cooling Rates FD 98342

For those cases, however, when all attempts were made to produce high quality yields, the results were encouraging. Ceramic reactivity during the melting and pouring cycles appeared insignificant by visual checks, physical measurements, and by optical and X-ray fluorescent indications during evaluation of the powder itself. Molten metal exposure times to the ceramic components have been short, naturally, and continued investigation is certainly in order. The low superheat circumstance and the low metal velocities through the nozzle, however, should assist greatly in preventing an irreversible condition of degradation by ceramic entrapment.

3000X FAL 86876

105μ - 177μ Particles

3000X FAL 86882

65μ - 105μ Particle

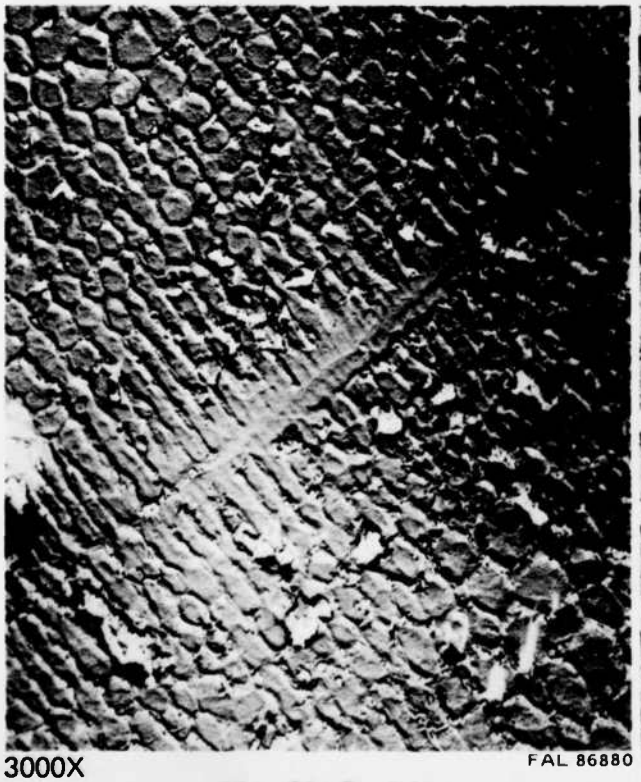

3000X FAL 86880

45μ - 65μ Particle

10,000X FAL 86873

<45μ Particle

Figure 26. Microstructure of IN100 Alloy Powder FD 98340

Simple sampling procedures are being prepared in order to provide statistical insurance that the methods used for analyzing inclusion content have reasonable reliability. The method to be employed involves compaction of the powder and subsequent cross-sectioning to expose large areas (relative to the powder) for study. For 50$\mu$ particles, for example, it should be possible to attain 99.9% confidence that the inclusion content is less than 10 ppm by analyzing 35 $cm^2$ per kilogram of material. This method will be used when inert handling capability is achieved.

Oxygen concentrations are being determined for the powders also since absolute control over $O_2$ pickup is considered essential to the success of the program. Less than 100 ppm $O_2$ has been set as a program goal. The remelt stock being used presently is running about 25-30 ppm $O_2$.

In runs made where instability was evident (such as failure of the atomizer surface), $O_2$ levels higher than 1000 ppm were determined for all powder size fractions. However, where stability was achieved, coarse powders ($\sim$150$\mu$) were found to contain less than 100 ppm, although the fine powder ($\sim$50$\mu$) showed $O_2$ levels in the 300-500 ppm range. Samples taken concurrently from the residual crucible skull exhibited levels on the order of 50-60 ppm $O_2$. These latter results with powder were considered reasonable since the measurements were made after exposure to the ambient environment and since similar measurements on superalloy powders purchased from suppliers who have consistently produced high quality material showed essentially the same results when tested in the same manner. The pickup of about 25 ppm $O_2$ in the residual skull from the remelt crucible was not expected, however, and present efforts are being made in an effort to determine why and to correct accordingly.